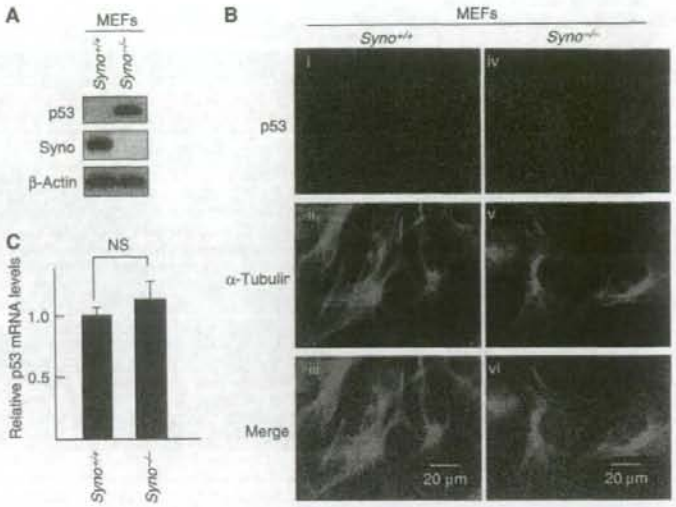

Figure 1 Accumulation of p53 in *synoviolin* null cells. (**A**) Accumulation of p53 in $Syno^{-/-}$ MEFs. (**B**) Nuclear accumulation of p53 in $Syno^{-/-}$ MEFs. p53 in $Syno^{+/+}$ MEFs (i–iii) and $Syno^{-/-}$ MEFs (iv–vi). Merged images are shown in the bottom panels (iii, vi). (**C**) Quantification of p53 mRNA. The *p53* mRNA level was assessed by real-time PCR and normalized to 18S rRNA. Data are mean ± s.e.m. of four experiments. Statistical analysis using Student *t*-test indicated no significant difference between $Syno^{+/+}$ and $Syno^{-/-}$ MEFs (NS).

apoptosis of synovial cells. These results indicate that Synoviolin is a novel causative factor for arthropathy based on its anti-apoptotic effects. In another study, we reported that all mice fetuses lacking *synoviolin* ($Syno^{-/-}$) died *in utero* around E13.5 (Yagishita *et al*, 2005), although Hrd1p/Del3p, a yeast ortholog of Synoviolin, was described as non-essential for survival. $Syno^{-/-}$ were anemic owing to enhanced apoptosis of fetal liver cells (Yagishita *et al*, 2005). It is surprising that an ER-associated degradation (ERAD)-associated E3 ubiquitin ligase, Synoviolin, is involved in cell hyperplasia of dividing cells via its anti-apoptotic effect. In this regard, like RSCs, the anti-apoptotic effect of Synoviolin was observed even for *synoviolin* expressed ectopically in NIH3T3 cells, which resulted in enhanced cell overgrowth in these cells (Tsuchimochi *et al*, 2005). These results were confirmed also in the *Drosophila* fly (Supplementary Figure 1). An important question remains unanswered at this stage. What is the mechanism of Synoviolin-induced cell overgrowth? The present study was designed to identify the substrates for Synoviolin that may be involved in cell growth.

Results

Accumulation of p53 in synoviolin-null cells

To identify target(s) for Synoviolin, we assumed that the lack of Synoviolin results in accumulation of substrate proteins. First, we carried out a two-dimensional polyacrylamide gel electrophoresis (PAGE) using mouse embryonic fibroblasts (MEFs) of $Syno^{-/-}$. In these experiments, p53 was identified as one of the major targets in the profile by LC-MAS analysis (Supplementary Figure 2). Indeed, the level of p53 was markedly enhanced in $Syno^{-/-}$ MEFs (Figure 1A) and $Syno^{-/-}$ embryos, especially in the posterior part of the body such as somites, brains and maxillary or branchial arches (Supplementary Figure 3), as reported previously (Gottlieb *et al*, 1997). The accumulated p53 was predominantly localized in the nuclei of $Syno^{-/-}$ MEFs (Figure 1B), although the mRNA level of *p53* was not altered in $Syno^{-/-}$ MEFs (Figure 1C). Phosphorylation of p53 was not observed in $Syno^{-/-}$ MEFs (Supplementary Figure 4).

Increment of functional p53 in synoviolin-null cells

Next, we tested whether impairment of Synoviolin influences the functions of p53 in the cell. Knockdown of Synoviolin by small interfering RNA (siRNA) for *synoviolin* (*Syno* siRNA) in RKO cells, a human colon cancer cell line known to express wild-type (WT) p53 (Smith *et al*, 1995), resulted in almost complete disappearance of Synoviolin expression (Figure 2A). Synoviolin knockdown was associated with increased p53 protein level and nuclear accumulation of p53 (Figure 2A and B), but no change in p53 mRNA levels (Figure 2C). No changes were noted in the expression levels of other ubiquitin ligases for p53 such as MDM2, Arf-BP (data not shown) and Parc (see Figure 4B), in *synoviolin*-null RKO cells (Brooks and Gu, 2006). On the other hand, the expression levels of unfolded protein response (UPR) markers such as HERP and PERK (Wu and Kaufman, 2006) were increased, which suggests that accumulation of unfolded proteins in *synoviolin*-knockdown RKO cells caused ER stress, followed by UPR (data not shown). These results were confirmed in other cell lines (HEK293 cells and HeLa cells, data not shown). In another experiment, a marked increase was noted in the binding of p53 to its consensus sequences such as *GADD45*, *MDM2* and *p21* promoter in *synoviolin*-knockdown cells compared with *GFP*-knockdown cells (Figure 2D). Furthermore, further additions of the respective competitor abrogated the binding capacity dose-dependently, confirming the specific interactions of p53 on electrophoretic mobility

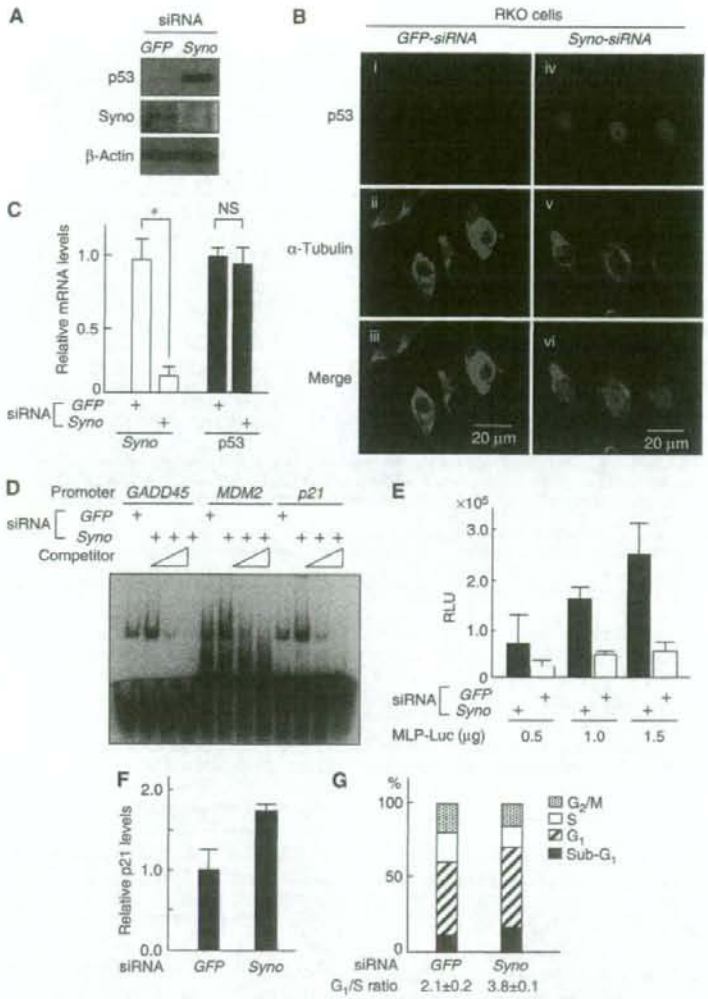

Figure 2 Functional evaluation of increased p53 in *synoviolin*-deficient RKO cells. (**A**) Increment of endogenous p53 by depletion of *synoviolin*. (**B**) Depletion of *synoviolin* causes nuclear accumulation of p53. Merged images are shown in the bottom panels (iii, vi). (**C**) *synoviolin* depletion does not affect mRNA levels of *p53*. Real-time PCR was performed as in Figure 1C. $^*P<0.01$. (**D**) DNA-binding activity of p53 for promoters of the indicated genes increases by depletion of *synoviolin*. (**E**) Transactivation activity of p53 is increased upon depletion of Synoviolin. Relative transactivation activity was determined by normalizing luciferase to an internal control, β-Gal activity from RSV-β-gal plasmid. RLU, relative light units. (**F**) siRNA depletion of *synoviolin* causes activation of p21 expression. (**G**) siRNA-induced depletion of *synoviolin* induces G_1 arrest. The cell-cycle profile was determined by propidium iodide staining and FACS. The results represent the average of triplicate experiments. Data in (C), (E) and (F) are mean ± s.e.m. of four experiments.

shift assay (EMSA) (Figure 2D). We also noted three times increment of luciferase activities on *GADD45*-MLP-Luciferase reporter plasmid in *synoviolin*-deficient RKO cells compared with *GFP*-siRNA-treated RKO cells (Figure 2E). Moreover, in *Syno* siRNA-treated RKO cells, we detected enhanced expression of p21, one of the target genes of p53 (Figure 2F), and the accumulation of cells in G_1 phase and decreased cells in S phase (Figure 2G). Taken together, the above results indicate that Synoviolin deficiency is not only associated with increased levels of p53, but also with functional activation of p53.

Synoviolin sequestrates p53 in the cytoplasm

To understand the molecular mechanism of Synoviolin-induced control of p53, we investigated the interaction between Synoviolin and p53 *in vitro*. As shown in Figure 3A, GST-SynoΔTM interacted directly with p53 (lane 8). A series of N-terminus Synoviolin-TM deletion mutants showed that the amino-acid sequence 236–270 of Synoviolin is responsible for binding with p53 (lanes 1–6) (this binding domain was termed provisionally as '53BD'). Furthermore, a synthetic 53BD peptide inhibited Synoviolin-p53 interaction in a dose-

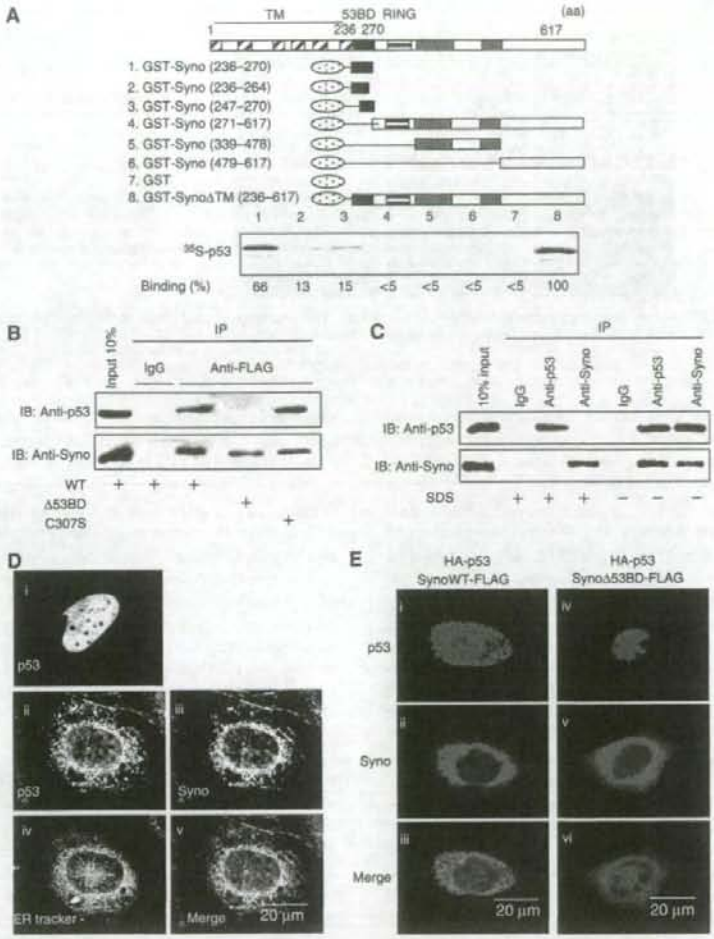

Figure 3 Synoviolin sequestrates p53 in the ER through its 53BD-dependent interaction with p53. (**A**) Identification of p53-binding domain of Synoviolin *in vitro*. Black box: p53-binding domain (53BD), gray box: proline-rich domain, oval box: GST. Relative binding ability is denoted as percentage (100% = SynoΔTM, lane 8). (**B**) 53BD-dependent *in vivo* binding of Synoviolin with p53 in HEK293 cell. (**C**) Interaction between endogenous Synoviolin and p53 in HEK293 cells. Cell lysates were immunoprecipitated in the presence or absence of SDS by using anti-p53 antibodies, anti-Synoviolin antibodies or control IgG. Inputs and immunoprecipitates were analyzed by Western blot by using anti-p53 or anti-Synoviolin antibodies. (**D**) P53 is anchored around ER in a Synoviolin-dependent manner. Saos-2 cells were transfected with HA-p53 (i) or co-transfected with HA-p53 and Synoviolin-FLAG (ii–v). Panel v shows a merged image with p53 (green), Synoviolin (red) and ER-Tracker stain (blue). (**E**) Binding of p53 with Synoviolin is required for p53 anchoring in the ER. Saos-2 cells were co-transfected with HA-p53 and Synoviolin WT-FLAG (i–iii) or SynoviolinΔ53BD-FLAG (iv–vi). Merged images are shown in the bottom panels (iii, vi).

dependent manner, whereas a peptide representing amino acids 322–332 of Synoviolin, used as a negative control, did not show any inhibitory activity (Supplementary Figure 5). We also confirmed *in vivo*, using co-immunoprecipitation assay, the interaction of transiently expressed exogenous Synoviolin WT-FLAG and p53, and the necessity of 53BD was also apparent (Figure 3B). The interaction of these two molecules was independent of ubiquitin ligase activity of Synoviolin, because Synoviolin C307S-FLAG lacking E3 activity bound to p53, as its WT (Figure 3B). Furthermore, endogenous interaction of p53 and Synoviolin was also confirmed in HEK293 cells (Figure 3C).

Considering the interplay between the ER-resident Synoviolin and the nuclear p53, we next investigated their cellular localization in Saos-2 cells, a human osteosarcoma cell line that lacks the endogenous p53 gene (Fogh *et al*, 1977), under conditions of transient expression of exogenous HA-p53 with Synoviolin WT-FLAG or SynoviolinΔ53BD-FLAG (Figure 3D and E). By overexpression of HA-p53 alone in these cells, HA-p53 was localized in the nucleus (Figure 3Di), as reported previously (Shaulsky *et al*, 1990). On the other hand, when HA-p53 was coexpressed with Synoviolin WT-FLAG, HA-p53 was predominantly colocalized with Synoviolin WT-FLAG in the perinuclear regions, but not in

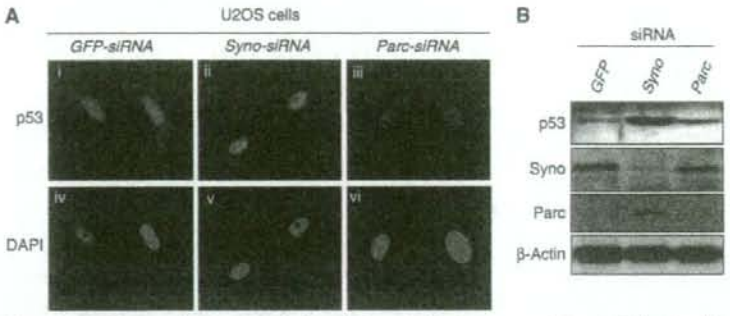

Figure 4 p53-related functional differences between Synoviolin and Parc. (**A**) Nuclear accumulation of p53 by knockdown of *synoviolin* or *Parc*. (**B**) Different levels of p53 following knockdown of *synoviolin* compared with *Parc*.

the nucleus (Figure 3Dii, iii and v). The perinuclear regions were confirmed to be the ER, by counterstaining with ER-Tracker Blue-White DPX (Figure 3Div and v). In addition, ectopically expressed SynoviolinΔ53BD-FLAG did not affect the translocation of HA-p53 into the nucleus (Figure 3E). These results clearly indicate that Synoviolin entraps p53 around ER, and that 53BD is required for this sequestration *in vivo*. In this regard, a previous study reported that another RING finger protein, Parc (Nikolaev *et al*, 2003), also acts as a cytoplasmic anchor for p53. To compare the characteristics of Synoviolin and Parc, we investigated p53 localization in U2OS cells, a human osteosarcoma cell line known to express WT p53 (Ponten and Saksela, 1967), after depletion of *synoviolin* or *Parc* (Nikolaev *et al*, 2003). Treatment with either *Syno* siRNA (Figure 4Aii and v) or *Parc* siRNA (Figure 4Aiii and vi) resulted in accumulation of p53 in the nucleus with diffused and lesser staining in the cytoplasm, different from treatment with *GFP* siRNA. Whereas the nuclear translocation of p53 was comparable in both *Syno* siRNA and *Parc* siRNA cells, a higher expression of p53 was observed in *synoviolin*-deficient U2OS cells (Figure 4Aii and iii). Western blotting analysis also revealed increased level of p53 in Synoviolin-knockdown but not in Parc-knockdown cells (Figure 4B). These findings indicate that Synoviolin regulates both localization and quantity of p53, whereas Parc does not affect the amount of p53, as reported previously (Nikolaev *et al*, 2003).

Synoviolin functions as a novel E3 ubiquitin ligase for p53 degradation

Considering that Synoviolin interacts with p53 *in vitro* and *in vivo*, we next examined whether Synoviolin ubiquitinates p53. As shown in Figure 5A, polyubiquitinated GST-p53 was detected only in the presence of ATP, PK-His-HA-Ub, E1, E2 (UbcH5c) and SynoviolinΔTM (SynoΔTM). This activity was not observed when we used Synoviolin with mutation in the RING finger domain (Figure 5B), and the deletion of 53BD also did not show any ubiquitination activity on p53 (Figure 5B), but this mutant by itself still preserved the auto-ubiquitination activity (Supplementary Figure 6). In addition, the 53BD peptide also inhibited poly-ubiquitination of p53 compared with a control peptide (amino acids 322–332), although the 53BD peptide did not influence the auto-ubiquitination activity of Synoviolin (Supplementary Figure 7). Moreover, ubiquitinated FLAG-p53 was observed when HA-tagged ubiquitin and Synoviolin WT were coexpressed in HEK293 cells because of its easy transfection, but Synoviolin C307S did not (Figure 5C). As a positive control, p53 was ubiquitinated by MDM2 in an *in vivo* ubiquitination assay (Figure 5C) (Haupt *et al*, 1997; Kubbutat *et al*, 1997).

In the next step, we tested the implication of ubiquitination of p53 by Synoviolin in the degradation of p53 *in vivo*. In HEK293 cells, overexpressed Synoviolin WT significantly shortened the half-life of endogenous p53, whereas Synoviolin C307S and SynoviolinΔ53BD did not increase the degradation rate of p53 (Figure 5D top, mock: 125.5 ± 18.2 min, Synoviolin WT: 44.8 ± 3.8 min, Synoviolin C307S: 177.3 ± 26.8 min and SynoviolinΔ53BD: 161.0 ± 41.4 min). These results indicate that Synoviolin is responsible for the turnover of p53 as its E3 ubiquitin ligase *in vivo*. Consistent with these data, the half-life of p53 was significantly prolonged in $Syno^{-/-}$ MEFs (Figure 5D (bottom), $Syno^{+/+}$ MEFs: 26.1 ± 1.6 min; and $Syno^{-/-}$ MEFs: 120.0 ± 30.3 min. $P<0.05$) as well as RKO cells treated with *synoviolin* siRNA (Supplementary Figure 8). In this regard, several ubiquitin ligases, such as *Cop1* (Dornan *et al*, 2004), *Pirh2* (Leng *et al*, 2003) and *MDM2* (Haupt *et al*, 1997; Kubbutat *et al*, 1997), are already reported to negatively regulate p53 (Bode and Dong, 2004). To ascertain the significance of Synoviolin relative to these ligases, we compared the effects of depletion of *synoviolin* and/or *Cop1*, *Pirh2* or *MDM2* on the expression level of p53 in RKO cells. The amount of p53 by *synoviolin* ablation was less than that by *MDM2* ablation, but equivalent to that by *Cop1* ablation. Depletion of *synoviolin* in cells treated with siRNA for *Cop1*, *Pirh2* or *MDM2* non-redundantly increased p53 levels (Figure 5E). Therefore, Synoviolin functionally targets p53 independent of other ubiquitin ligase pathways. Then, does Synoviolin regulate p53 activation process? To address this question, we applied genotoxic stress as a stimulus for p53 activation (Kastan *et al*, 1991; Vogelstein *et al*, 2000). *Syno* siRNA and *GFP* siRNA-transfected RKO cells were treated with or without genotoxic stresses such as camptothecin, actinomycin D and γ-irradiation. As expected, increased level of p53 by Synoviolin knockdown was cooperatively enhanced by treatment with genotoxic stresses in these cells (Figure 5F). Thapsigargin induced Synoviolin expression, as reported previously (Yagishita *et al*, 2005),

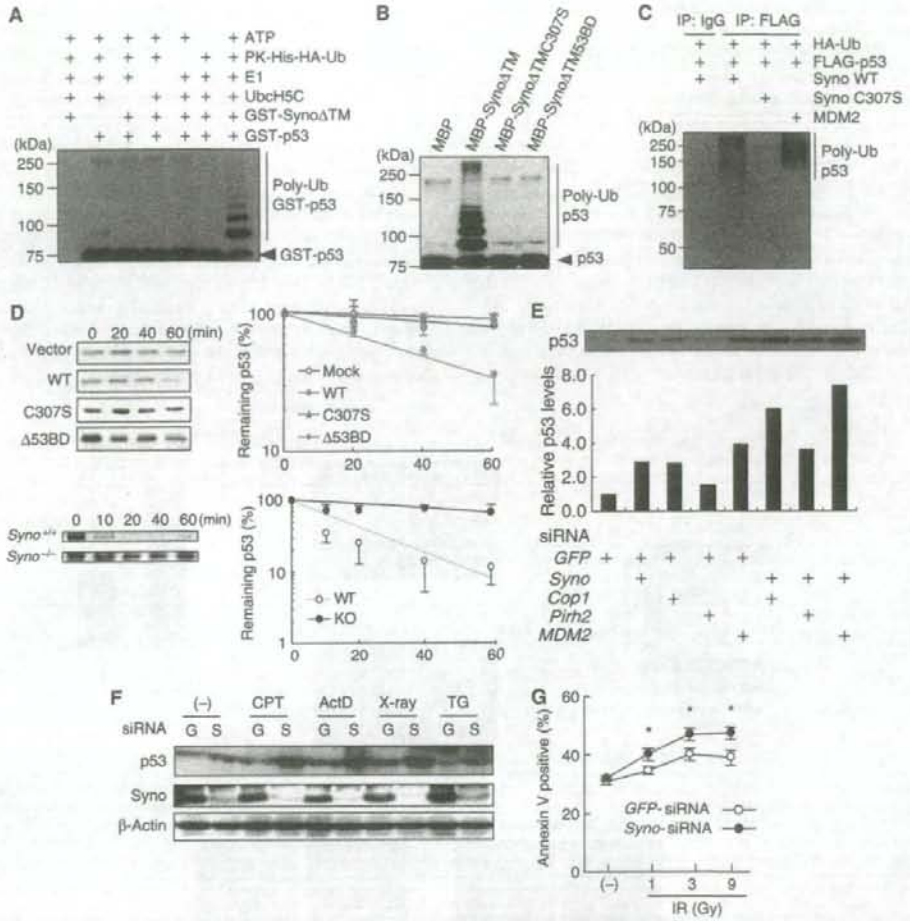

Figure 5 Synoviolin up-regulates p53 level in cells under normal and genotoxic stress conditions. (**A**) Synoviolin ubiquitinates p53 *in vitro*. (**B**) The ubiquitination of p53 is dependent on an intact RING finger domain. (**C**) WT Synoviolin, but not RING finger mutant, ubiquitinates p53 *in vivo*. (**D**) Synoviolin over-expression in HEK293 cells increases degradation of p53 (top). At 24 h after the transfection with empty vector, wild type Synoviolin (WT), mutants in RING finger domain (C307S) or p53 binding domain deletion mutant (Δ53BD), p53 expression was examined at indicated time of cycloheximide treatment. Degradation of p53 is inhibited in synoviolin knockout MEFs ($Syno^{-/-}$) compared with wild type MEFs ($Syno^{+/+}$). The p53 expression was examined after the indicated time of cycloheximide treatment. The remaining p53 expressions were normalized to β-actin expression and plotted against time (minutes). (**E**) Effects of knockdown of Synoviolin and/or other known E3 ubiquitin ligases for p53 on the level of p53 in RKO cells. Quantified p53 level is expressed as relative levels (1.0 = *GFP*-siRNA treated RKO cells). (**F**) Genotoxic stress induces p53 accumulation in the absence of Synoviolin. *GFP*- siRNA (G). *syno* siRNA (S). At 48 h after transfection, the RKO cells were treated with vehicle, camptothecine (CPT, 0.5 μM), actinomycin D (ActD, 5 nM), X-Ray (9 Gray) or thapsigargin (TG, 1 μM) for 6 h. (**G**) Synoviolin knockdown sensitizes cells to genotoxic stress. At 48 h after transfection, cells were exposed to the indicated doses of ionizing-radiation for 24 h, followed by FACS analysis to detect annexin V-positive cells. Data in (D) and (G) are mean ± s.e.m. of $n \geqslant 3$. $^*P < 0.05$.

which was abolished in *Syno* siRNA-transfected RKO cells (Figure 5F). Consistent with the findings of a previous report (Qu *et al*, 2004), thapsigargin, an ER stress inducer, destabilized p53 expression compared with vehicle treatment in *GFP* siRNA-treated RKO cells. Interestingly, the thapsigargin-induced inhibition of p53 expression was reversed, at least in part, by the ablation of Synoviolin (Figure 5F). In addition, the sensitivity of *syno* siRNA-treated RKO cells to γ-irradiation was significantly increased compared with *GFP* siRNA-treated RKO cells (Figure 5G). Considered together, these results indicate that Synoviolin also participates in genotoxic stress response through the mechanism identified here.

Synoviolin regulates p53-dependent apoptotic pathway in vivo

The above experiments provided several pieces of evidence that Synoviolin is a novel class of E3 ubiquitin ligase for p53. However, the majority of the results obtained from cultured cells may not fully reflect the physiological function of p53 in

the context of the whole organism. Therefore, we used *Drosophila* to confirm the association between Synoviolin and p53. Among *Drosophila* clones, CG1937 was identified by BLASTP (protein–protein blast analysis using flybase—http://flybase.bio.indiana.edu/blast/) as the gene with 63% homology to mammalian Synoviolin, and the RING domain of CG1937 is highly conserved (82%) and *in vitro* ubiquitination assay evidently indicated that *Drosophila* Synoviolin (dSyno) ubiquitinates *Drosophila* p53 (Dmp53) (Figure 6A) (Ollmann *et al*, 2000). To investigate the role of Synoviolin in p53 regulation in the whole organism, we generated transgenic flies in which Dmp53 or dSyno was overexpressed by tissue-specific Gal4 driver (Harrison *et al*, 1995). By crossing each transgenic fly, we generated e16E-Gal4/UAS-Dmp53;UAS-dSyno/+ flies, in which both Dmp53 and dSyno could be overexpressed in the posterior halves of wings by e16E-Gal4 driver. The expression level of Dmp53 in the wing discs was significantly decreased in e16E-Gal4/UAS-Dmp53;UAS-dSyno/+ discs compared with e16E-Gal4/Dmp53;+/+ discs (Figure 6B). Moreover, acridine orange staining of apoptotic cells in these discs demonstrated that the level of apoptosis induced by overexpression of Dmp53 was diminished by dSyno overexpression (Figure 6C). These results indicate that dSyno affects Dmp53 protein levels in the fly system, similar to the results of the cell culture system.

In addition to decreased Dmp53 protein level by dSyno in the wing discs of adult flies, dSyno altered the wing phenotype. Namely, overexpression of Dmp53 by e16E-Gal4 driver caused bubbled wing phenotype at the posterior half of wings (Figure 6Di). This phenotype was completely suppressed by dSyno overexpression (Figure 6Dii and Supplementary Table 1). Overexpression of dSyno alone by e16E-Gal4 driver also produced wing phenotype (weak wrinkling of the posterior edge of the wing) (Figure 6Diii). This wrinkled phenotype

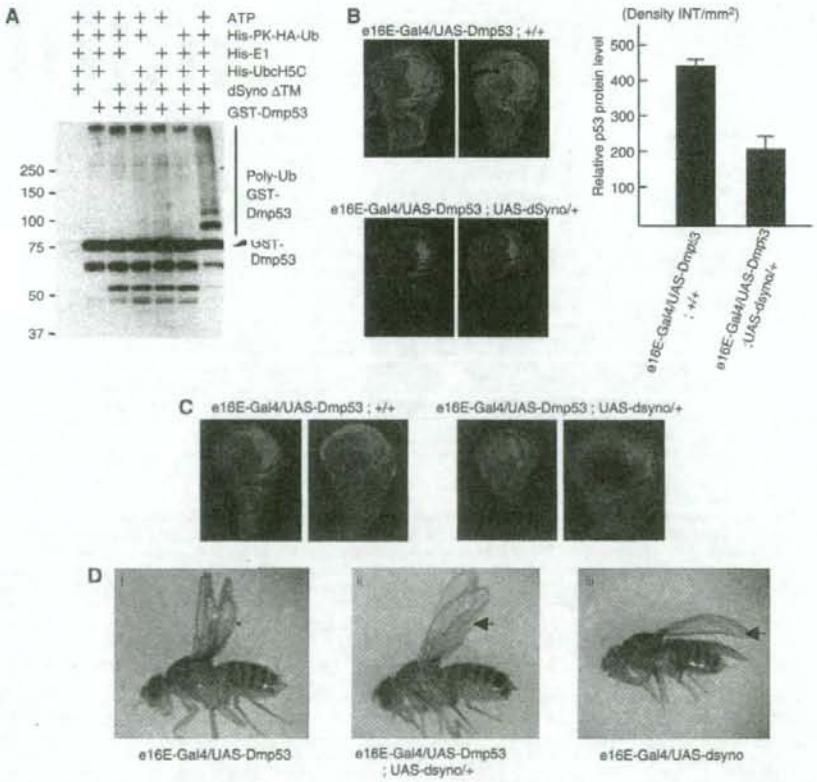

Figure 6 Synoviolin directly regulates p53-dependent apoptotic pathway in *Drosophila* fly. (**A**) Fly homolog of Synoviolin ubiquitinates fly homolog of p53 *in vitro*. GST-fusion *Drosophila melanogaster* p53 (Dmp53) was incubated with or without ATP, His-PK-HA-Ub, His-E1 (human), His-UbcH5C (human) and *Drosophila* Synoviolin (dSyno)ΔTM. Ubiquitinated proteins were probed with anti-HA antibody. (**B**) P53 protein level of wing discs was determined by immunostaining using anti-Dmp53 antibody (left). 2 representative pictures of each fly are shown. The fluorescence intensity of each 15 fly disc was quantified, and the net density level (Density INT/mm^2) was determined by subtracting the density level of the background area (anterior half of disc) from the measured level of the target area (posterior half of disc) (right). Data are mean ± s.e.m. of $n = 15$. (**C**) Apoptosis was examined by Acridine orange staining of wing disc. Overexpression of dSyno in the posterior half of the discs reduced Dmp53 overexpression-induced apoptosis. (**D**) Overexpression of dSyno suppressed the Dmp53-induced bubbled wing phenotype. The extent of wing bubble (*) in e16E-Gal4/UAS-Dmp53 flies varied with age, but the penetrance of bubbled wing phenotype was close to 100% (Supplementary Table 1). Overexpression of dSyno suppressed the Dmp53-induced bubbled wing phenotype, but dSyno-induced wrinkled phenotype at the posterior edge of wing was still observed (arrow).

induced by dSyno overexpression was not affected by Dmp53 in the double overexpressing flies (Figure 6Dii and iii, arrow). These results confirm that dSyno regulates Dmp53 protein level *in vivo* and such regulation might be accomplished through ubiquitination of dDmp53.

To determine whether this phenotypic suppression of Dmp53 by dSyno is specific to Dmp53, we investigated the interaction between dSyno and the upstream activators of p53 such as dATM, CHK2, using the same strategy. None of these activators showed interaction with dSyno (data not shown), suggesting that dSyno regulates Dmp53 protein level directly *in vivo*.

Discussion

We provide concrete evidence for the first time of the functional relationship between Synoviolin and p53. As a target for Synoviolin, p53 is evidently a non-ERAD substrate. In this regard, Doa10p, the RING finger E3 ubiquitin ligase, is known not only to be involved exclusively in removing ER proteins in the ERAD, but also to eliminate cytoplasmic targets, especially the soluble transcriptional factor Matα2, which translocates into the nucleus similar to p53 (Swanson *et al*, 2001; Laney and Hochstrasser, 2003). Thus, our finding can be viewed within the same framework of yeast though in higher eukaryotes. In the meantime, it was proposed that the ERAD in yeast is composed of two distinct surveillance mechanisms, that is, the folded state of luminal domains and the cytosolic domains are monitored by ERAD-luminal (ERAD-L) and ERAD-cytosolic (ERAD-C) pathways, respectively (Vashist and Ng, 2004; Nishikawa *et al*, 2005). Hrd1p is recognized as an ERAD-L ligase; however, this classification is not applicable to Synoviolin as a human homolog of yeast Hrd1, because Synoviolin can target both ERAD-L substrate and cytoplasmic p53 (ERAD-C substrate). Therefore, we propose the novel regulatory system of Synoviolin as a different classification of the ERAD-L/C pathway.

Maintenance of homeostasis is an important cellular function, and cells are equipped with various processes to maintain their conditions. Transcriptional alteration mediated by p53 results in a variety of cell fate changes, including growth arrest and apoptosis (Vousden and Lu, 2002; Meek, 2004). Normally, the cell maintains low levels of p53 through rapid protein degradation via the UPS by the function of ubiquitin ligases. In contrast, under genotoxic stress conditions, stabilization of p53 is promoted and the diffusely distributed p53 translocates to the nucleus owing to growth inhibition and apoptosis by its transcriptional activity. Thus, adjusting the level and nuclear localization of p53 are two essential processes for cells in order to maintain the physiological state. Although p53 mutations have been documented in more than half of all human tumors (Hollstein *et al*, 1999), it is also known that tumor cells retain WT p53. In this regard, functional inactivation of WT p53 by abnormal cytoplasmic sequestration is frequently observed in many tumor types (Moll *et al*, 1992, 1996; Schlamp *et al*, 1997). The RING finger protein Parc is considered to act as a cytoplasmic anchoring molecule of p53, but this clone does not have a p53 ubiquitination activity (Nikolaev *et al*, 2003). On the other hand, our present findings demonstrated that Synoviolin not only anchors p53 in the cytoplasm, but also ubiquitinates it, and thus differs from Parc (Figure 4). Moreover, Synoviolin diverges from other ligases for p53; each of the three ubiquitin ligases for p53 (MDM2, Pirh2 and Cop1) forms an autoregulatory negative feedback loop, resulting in lower p53 activity upon its expression, but these three ligases are target for the p53 transcriptional pathway (Dornan *et al*, 2004; Leng *et al*, 2003), whereas the expression of Synoviolin is not regulated by p53 (Figure 5F). Indeed, the *synoviolin* promoter region does not have a p53 target sequence, whereas it contains the ER stress responsive element (Tsuchimochi *et al*, 2005) and responds to the stress (Figure 5F). The reason for the multiple post-translational steps for p53 is the enormous importance of this molecule in maintaining cellular homeostasis. p53 is negatively regulated by various ubiquitin ligases, such as MDM2, MdmX, HAUSP, ARF, COP1, Pirh2 and ARF-BP1 (Brooks and Gu, 2006), and it is assumed that each molecule has its specific roles in p53 control. Among them, Synoviolin is also a unique regulator of p53 because of its independency from other ligases and transcriptional regulation by p53, ER localization and canonical function in ERAD.

In the present study, we demonstrated that Synoviolin participates in genotoxic stress-mediated p53 signaling, and its to participation in the ER stress-induced apoptosis is also well known (Bordallo *et al*, 1998; Kaneko *et al*, 2002; Kikkert *et al*, 2004; Yagishita *et al*, 2005). Therefore, Synoviolin seems to regulate two distinct apoptotic pathways and the ubiquitination of p53 by Synoviolin may be another target for crosstalk between them. Another linkage between ER stress and p53 pathway is also implicated by our finding that UPR markers are increased in cells with *synoviolin* knockdown (data not shown). Two reports described a crosstalk of p53- and ER stress- induced apoptosis pathways, that is, ER stress antagonizes p53-mediated apoptosis through the cytoplasmic localization of p53 due to phosphorylation by glycogen synthase kinase-3β (GSK-3β) (Qu *et al*, 2004), and p53 destabilization utilized the cooperative action of MDM2 and GSK-3β in ER-stressed cells (Pluquet *et al*, 2005). In this regard, it is important to note that UPR activation upon Synoviolin knockdown in RKO cells may be related to ER stress with impaired ERAD system. Since Synoviolin null cells show upregulation of p53, it is possible that the effect of p53 stabilization by Synoviolin knockdown exceeds the p53 destabilization effect of UPR induced by Synoviolin knockdown. This hypothesis may be supported by the finding that *synoviolin* siRNA treatment seemed to restore the expression of p53 at least in part, which was suppressed by ER stress (Figure 5F). The regulatory action of Synoviolin on p53 under ER stress is obviously more complex, because ER stress also induces Synoviolin expression. Further studies are necessary to determine the physiological regulatory role of Synoviolin in p53 expression under ER stress conditions.

The function of p53 in patients with RA is still controversial (Firestein *et al*, 1997; Reme *et al*, 1998; Inazuka *et al*, 2000; Muller-Ladner and Nishioka, 2000; Sun and Cheung, 2002). Mice lacking p53 do not develop spontaneous arthropathy but have severe collagen-induced arthritis (CIA) (Yamanishi *et al*, 2002; Simelyte *et al*, 2005). As we reported previously, overexpression of Synoviolin resulted in spontaneous arthropathy and its deficiency resulted in resistance to CIA in mice (Amano *et al*, 2003). Therefore, we assumed that the severity of arthritis could be determined by the Synoviolin–p53 control pathway and that the onset of spon-

taneous arthropathy may be caused by p53-independent pathway in these models. The influence of these relationships on arthritis is currently being examined in our laboratories, using *synoviolin* and p53 double null mutant mice. We hope that our research could uncover new pathogenic mechanisms of RA. Furthermore, since p53 is an important tumor suppressor gene, we believe that Synoviolin could be a useful therapeutic target for not only RA but also cancer based on its cytological and biochemical features, i.e., cytoplasmic localization and enzymatic activity (Hopkins and Groom, 2002).

In conclusion, we demonstrated that Synoviolin acts as an ERAD E3 ubiquitin ligase that controls cellular p53 and thus opens, a new concept for proliferative disorders such as RA and cancer.

Materials and methods

Plasmids

pcDNA3/Synoviolin WT or C307S-FLAG, pcDNA3/HA- and FLAG-p53, pcDNA3/MDM2 and pcDNA/HA-Ub plasmids have been described previously (Amano *et al*, 2003; Matsushita *et al*, 2005). Deletion of 53BD, MBP- and GST-fusions in Synoviolin deletion mutants was performed by PCR-based method in this study. To clone a cDNA encoding *Drosophila* homolog of human Synoviolin (dSyno), 2282 bp of CG1937 was cut out from EST GH11117 with *EcoRI*/*XhoI*, and subcloned into pUAST vector (Brand and Perrimon, 1993). The sequences of all plasmids generated by PCR were confirmed by ABI auto-sequencer.

Cells and transfections

RKO and HEK293 cells were cultured in Minimum Essential Medium (Sigma) and U2OS and Saos-2 in Dulbecco's modified Eagle's medium (Sigma). The sense sequences of siRNA oligonucleotides to *synoviolin* are (1) GGUGUUCUUUGGGCAACUG, (2) GCUGUGACAGAUGCCAUCA, (3) GGUUCUGCUGUACAUGGCC. Changes in p53 protein in RKO cells were determined by all these siRNAs. The sense sequence of siRNA oligonucleotides to *GFP* is GGCUACGUCCAGGAGCGC.

GST pull-down assay

GST-fusion proteins were expressed in *Escherichia coli* strain BL21 (Invitrogen) and purified by using glutathione-Sepharose beads (Amersham Biosciences). *In vitro*-translated ^{35}S-labeled p53 was pre-cleaned with 10 μg GST protein for 1 h at 4°C, followed by incubation with 10 μg of each GST-fusion protein in binding buffer (20 mM *N*-2-hydroxyethylpiperazine-*N*'-ethanesulfonic acid (HEPES), pH 7.9, 150 mM NaCl and 0.2% TritonX-100) for 1 h at 4°C. After washing, bound proteins were separated by SDS–PAGE and detected by BAS.

Immunoprecipitation assay

For co-immunoprecipitation assay between exogenous Synoviolin and exogenous p53, HEK293 cells were co-transfected with HA-p53 and pcDNA3-Synoviolin WT-FLAG, pcDNA3-SynoviolinΔ53BD-FLAG or pcDNA3-Synoviolin C307S-FLAG plasmids. Cell extracts were prepared with high-salt buffer (20 mM HEPES pH 7.2, 420 mM NaCl, 10% glycerol, 0.5% NP-40, 0.5 mM dithiothreitol (DTT), and 1 mM phenylmethylsulfonyl fluoride (PMSF)) and diluted at three-fold with 0.5 mM DTT and a protease inhibitor solution, followed by incubation with mouse IgG or anti-FLAG antibody. Precipitated proteins were detected by anti-HA or anti-FLAG antibodies.

To detect the interaction between endogenous Synoviolin and p53, HEK293 cells were lysed in 100 mM Tris–HCl, 80 mM NaCl, 1 mM EDTA, 5 mM EGTA, 5% glycerol, 2% (w/v) digitonin, 0.1% Brij 35, protease inhibitor cocktail and 20 μM of MG132. Immunoprecipitation was carried out in the presence or absence of SDS by using anti-p53 antibodies, anti-Synoviolin antibodies or control IgG. The immunoprecipitated samples were analyzed by western blot by using anti-p53 or anti-Synoviolin antibodies.

In vitro and in vivo ubiquitination assays

The *in vitro* ubiquitination assay was conducted as described previously (Amano *et al*, 2003). For the peptide inhibition assay, reaction solutions lacking no MBP-SynoviolinΔTM-6xHis and ATP were incubated with 53BD or control peptides (50, 100, and 200 μM) for 30 min at 4°C. Reactions were started by addition of MBP-SynoviolinΔTM-6xHis and ATP and incubating at 37°C.

For the *in vivo* ubiquitination assay, HEK293 cells were transfected with pcDNA3/HA-Ubiquitin, pcDNA3/FLAG-p53, and pcDNA3/Synoviolin WT, C307S or pcDNA3/MDM2. At 24 h post-transfection, cells were treated with MG132 (10 μM) for 1 h, then the cells were lysed in SDS containing buffer (50 mM Tris, pH 7.5, 0.5 mM EDTA, 1% SDS, and 1 mM DTT) and boiled for 5 min to denature the proteins. The denatured samples were diluted with immunoprecipitation buffer (50 mM Tris, pH 7.5, 2 mM EDTA, 150 mM NaCl, and 0.1% NP-40 and protease inhibitor cocktail) and the p53 protein was immunopurified by using anti-p53 antibody. Ubiquitinated p53 was detected by western blotting by using anti-HA antibody.

Immunostaining of fly wing discs

Fly wing discs were dissected in PBS, fixed in a buffer containing 50 mM Tris–HCl, pH 6.8, 1 mM EGTA, 1% Triton ×-100, 2 mM $MgSO_4$, 150 mM NaCl, and 2.2% formaldehyde for 15 min, and blocked using a blocking buffer (50 mM Tris–HCl, pH 6.8, 150 mM NaCl, 0.5% NP-40 and 5 mg/ml BSA). The fixed wing discs were incubated overnight at 4°C in a 1:200 dilution of anti-Dmp53 (d-200) antibody. After washing in a wash buffer (50 mM Tris–HCl, pH 6.8, 150 mM NaCl, 0.5% NP-40 and 1 mg/ml BSA), they were incubated for 3 h at 4°C in donkey anti-rabbit FITC at 1:200 dilution, washed with the wash buffer and then mounted in a mounting solution (50 mM Tris–HCl, pH 6.8, 30% glycerol, 150 mM NaCl, and 5 mg/ml phenylethylendiamine). The fluorescence intensity of each disc was quantified with Quantity One software (Bio-Rad Laboratories). Acridine orange staining was performed as reported previously (Brodsky *et al*, 2000).

Supplementary data

Supplementary data are available at *The EMBO Journal* Online (http://www.embojournal.org).

Acknowledgements

We are grateful to MR Montminy, G Verdine, R Nagata, H Shimizu, I Hishinuma, H Yokohama, H Kato, S Kitamura, K Yoshimatsu, Yuichiro ITAKURA OFFICE and ES Takagi, for advice and encouragement, and to H Takahashi, M Sato, S Otani, A Sugamiya, N Takagi, S Shinkawa, Y Nakagawa, Y Sato, M Yamanashi and members of Toshi's Laboratory for the excellent technical assistance. This study was supported in part by LocomoGene Inc., Eisai Co., Ltd, National Institute of Biomedical Innovation, the Japanese Ministry of Education, Culture, Sports, Science and Technology, the Japanese Ministry of Health, Labour and Welfare, the Kato Memorial Trust for Nanbyo Research, the Japan Medical Association, Nagao Memorial Fund, Kanae Foundation for Life & Socio-medical Science, Japan Research Foundation for Clinical Pharmacology, Kanagawa Nanbyo Foundation, Kanagawa Academy of Science and Technology Research Grants, Japan College of Rheumatology, the Nakajima Foundation, Japan Society for Promotion of Science, New Energy and Industrial Technology Development Organization, Mochida Pharmaceutical Co. Ltd, Kanto Bureau of Economy, Trade and Industry, and the Uehara Memorial Foundation. HF is supported by Japan Society for the Promotion of Science.

References

Amano T, Yamasaki S, Yagishita N, Tsuchimochi K, Shin H, Kawahara K, Aratani S, Fujita H, Zhang L, Ikeda R, Fujii R, Miura N, Komiya S, Nishioka K, Maruyama I, Fukamizu A, Nakajima T (2003) Synoviolin/Hrd1, an E3 ubiquitin ligase, as a novel pathogenic factor for arthropathy. *Genes Dev* **17**: 2436–2449

Bode AM, Dong Z (2004) Post-translational modification of p53 in tumorigenesis. *Nat Rev Cancer* **4**: 793–805

Bordallo J, Plemper RK, Finger A, Wolf DH (1998) Der3p/Hrd1p is required for endoplasmic reticulum-associated degradation of misfolded lumenal and integral membrane proteins. *Mol Biol Cell* **9:** 209–222

Brand AH, Perrimon N (1993) Targeted gene expression as a means of altering cell fates and generating dominant phenotypes. *Development* **118:** 401–415

Brodsky MH, Nordstrom W, Tsang G, Kwan E, Rubin GM, Abrams JM (2000) *Drosophila* p53 binds a damage response element at the reaper locus. *Cell* **101:** 103–113

Brooks CL, Gu W (2006) p53 ubiquitination: Mdm2 and beyond. *Mol Cell* **21:** 307–315

Dornan D, Wertz I, Shimizu H, Arnott D, Frantz GD, Dowd P, O'Rourke K, Koeppen H, Dixit VM (2004) The ubiquitin ligase COP1 is a critical negative regulator of p53. *Nature* **429:** 86–92

Firestein GS, Echeverri F, Yeo M, Zvaifler NJ, Green DR (1997) Somatic mutations in the p53 tumor suppressor gene in rheumatoid arthritis synovium. *Proc Natl Acad Sci USA* **94:** 10895–10900

Fogh J, Wright WC, Loveless JD (1977) Absence of HeLa cell contamination in 169 cell lines derived from human tumors. *J Natl Cancer Inst* **58:** 209–214

Gottlieb E, Haffner R, King A, Asher G, Gruss P, Lonai P, Oren M (1997) Transgenic mouse model for studying the transcriptional activity of the p53 protein: age- and tissue-dependent changes in radiation-induced activation during embryogenesis. *EMBO J* **16:** 1381–1390

Harrison DA, Binari R, Nahreini TS, Gilman M, Perrimon N (1995) Activation of a *Drosophila* Janus kinase (JAK) causes hematopoietic neoplasia and developmental defects. *EMBO J* **14:** 2857–2865

Haupt Y, Maya R, Kazaz A, Oren M (1997) Mdm2 promotes the rapid degradation of p53. *Nature* **387:** 296–299

Hershko A, Ciechanover A (1998) The ubiquitin system. *Annu Rev Biochem* **67:** 425–479

Hollstein M, Hergenhahn M, Yang Q, Bartsch H, Wang ZQ, Hainaut P (1999) New approaches to understanding p53 gene tumor mutation spectra. *Mutat Res* **431:** 199–209

Hopkins AL, Groom CR (2002) The druggable genome. *Nat Rev Drug Discov* **1:** 727–730

Inazuka M, Tahira T, Horiuchi T, Harashima S, Sawabe T, Kondo M, Miyahara H, Hayashi K (2000) Analysis of p53 tumour suppressor gene somatic mutations in rheumatoid arthritis synovium. *Rheumatology* **39:** 262–266

Kaneko M, Ishiguro M, Niinuma Y, Uesugi M, Nomura Y (2002) Human HRD1 protects against ER stress-induced apoptosis through ER-associated degradation. *FEBS Lett* **532:** 147–152

Kastan MB, Onyekwere O, Sidransky D, Vogelstein B, Craig RW (1991) Participation of p53 protein in the cellular response to DNA damage. *Cancer Res* **51:** 6304–6311

Kikkert M, Doolman R, Dai M, Avner R, Hassink G, vanVoorden S, Thanedar S, Roitelman J, Chau V, Wiertz E (2004) Human HRD1 is an E3 ubiquitin ligase involved in degradation of proteins from the endoplasmic reticulum. *J Biol Chem* **279:** 3525–3534

Kubbutat MH, Jones SN, Vousden KH (1997) Regulation of p53 stability by Mdm2. *Nature* **387:** 299–303

Laney JD, Hochstrasser M (2003) Ubiquitin-dependent degradation of the yeast Mat(alpha)2 repressor enables a switch in developmental state. *Genes Dev* **17:** 2259–2270

Leng RP, Lin Y, Ma W, Wu H, Lemmers B, Chung S, Parant JM, Lozano G, Hakem R, Benchimol S (2003) Pirh2, a p53-induced ubiquitin-protein ligase, promotes p53 degradation. *Cell* **112:** 779–791

Matsushita N, Kitao H, Ishiai M, Nagashima N, Hirano S, Okawa K, Ohta T, Yu DS, McHugh PJ, Hickson ID, Venkitaraman AR, Kurumizaka H, Takata M (2005) A FancD2-Monoubiquitin Fusion Reveals Hidden Functions of Fanconi Anemia Core Complex in DNA Repair. *Mol Cell* **19:** 841–847

Meek DW (2004) The p53 response to DNA damage. *DNA Repair* **3:** 1049–1056

Moll UM, Ostermeyer AG, Haladay R, Winkfield B, Frazier M, Zambetti G (1996) Cytoplasmic sequestration of wild-type p53 protein impairs the G1 checkpoint after DNA damage. *Mol Cell Biol* **16:** 1126–1137

Moll UM, Riou G, Levine AJ (1992) Two distinct mechanisms alter p53 in breast cancer: mutation and nuclear exclusion. *Proc Natl Acad Sci USA* **89:** 7262–7266

Muller-Ladner U, Nishioka K (2000) p53 in rheumatoid arthritis: friend or foe? *Arthritis Res* **2:** 175–178

Nikolaev AY, Li M, Puskas N, Qin J, Gu W (2003) Parc: a cytoplasmic anchor for p53. *Cell* **112:** 29–40

Nishikawa S, Brodsky JL, Nakatsukasa K (2005) Roles of molecular chaperones in endoplasmic reticulum (ER) quality control and ER-associated degradation (ERAD). *J Biochem* **137:** 551–555

Ollmann M, Young LM, Di Como CJ, Karim F, Belvin M, Robertson S, Whittaker K, Demsky M, Fisher WW, Buchman A, Duyk G, Friedman L, Prives C, Kopczynski C (2000) *Drosophila* p53 is a structural and functional homolog of the tumor suppressor p53. *Cell* **101:** 91–101

Pickart CM (2001) Mechanisms underlying ubiquitination. *Annu Rev Biochem* **70:** 503–533

Pluquet O, Qu L, Baltzis D, Koromilas AE (2005) Endoplasmic reticulum stress accelerates p53 degradation by the cooperative actions of Hdm2 and Glycogen synthase kinase 3β. *Mol Cell Biol* **25:** 9392–9405

Ponten J, Saksela E (1967) Two established *in vitro* cell lines from human mesenchymal tumours. *Int J Cancer* **2:** 434–447

Qu L, Huang S, Baltzis D, Rivas-Estilla AM, Pluquet O, Hatzoglou M, Koumenis C, Taya Y, Yoshimura A, Koromilas AE (2004) Endoplasmic reticulum stress induces p53 cytoplasmic localization and prevents p53-dependent apoptosis by a pathway involving glycogen synthase kinase-3beta. *Genes Dev* **18:** 261–277

Reme T, Travaglio A, Gueydon E, Adla L, Jorgensen C, Sany J (1998) Mutations of the p53 tumour suppressor gene in erosive rheumatoid synovial tissue. *Clin Exp Immunol* **111:** 353–358

Schlamp CL, Poulsen GL, Nork TM, Nickells RW (1997) Nuclear exclusion of wild-type p53 in immortalized human retinoblastoma cells. *J Natl Cancer Inst* **89:** 1530–1536

Shaulsky G, Goldfinger N, Ben-Ze'ev A, Rotter V (1990) Nuclear accumulation of p53 protein is mediated by several nuclear localization signals and plays a role in tumorigenesis. *Mol Cell Biol* **10:** 6565–6577

Shearer AG, Hampton RY (2004) Structural control of endoplasmic reticulum-associated degradation: effect of chemical chaperones on 3-hydroxy-3-methylglutaryl-CoA reductase. *J Biol Chem* **279:** 188–196

Shearer AG, Hampton RY (2005) Lipid-mediated, reversible misfolding of a sterol-sensing domain protein. *EMBO J* **24:** 149–159

Simelyte E, Rosengren S, Boyle DL, Corr M, Green DR, Firestein GS (2005) Regulation of arthritis by p53: Critical role of adaptive immunity. *Arthritis Rheum* **52:** 1876–1884

Smith ML, Chen IT, Zhan Q, O'Connor PM, Fornace Jr AJ (1995) Involvement of the p53 tumor suppressor in repair of u.v.-type DNA damage. *Oncogene* **10:** 1053–1059

Sun Y, Cheung HS (2002) p53, proto-oncogene and rheumatoid arthritis. *Semin Arthritis Rheum* **31:** 299–310

Swanson R, Locher M, Hochstrasser M (2001) A conserved ubiquitin ligase of the nuclear envelope/endoplasmic reticulum that functions in both ER-associated and Matalpha2 repressor degradation. *Genes Dev* **15:** 2660–2674

Tsuchimochi K, Yagishita N, Yamasaki S, Amano T, Kato Y, Kawahara K, Aratani S, Fujita H, Ji F, Sugiura A, Izumi T, Sugamiya A, Maruyama I, Fukamizu A, Komiya S, Nishioka K, Nakajima T (2005) Identification of a crucial site for synoviolin expression. *Mol Cell Biol* **25:** 7344–7356

Vashist S, Ng DT (2004) Misfolded proteins are sorted by a sequential checkpoint mechanism of ER quality control. *J Cell Biol* **165:** 41–52

Vogelstein B, Lane D, Levine AJ (2000) Surfing the p53 network. *Nature* **408:** 307–310

Vousden KH, Lu X (2002) Live or let die: the cell's response to p53. *Nat Rev Cancer* **2:** 594–604

Wu J, Kaufman RJ (2006) From acute ER stress to physiological roles of the Unfolded Protein Response. *Cell Death Differ* **13:** 374–384

Yagishita N, Ohneda K, Amano T, Yamasaki S, Sugiura A, Tsuchimochi K, Shin H, Kawahara K, Ohneda O, Ohta T, Tanaka S, Yamamoto M, Maruyama I, Nishioka K, Fukamizu A, Nakajima T (2005) Essential role of synoviolin in embryogenesis. *J Biol Chem* **280:** 7909–7916

Yamanishi Y, Boyle DL, Pinkoski MJ, Mahboubi A, Lin T, Han Z, Zvaifler NJ, Green DR, Firestein GS (2002) Regulation of joint destruction and inflammation by p53 in collagen-induced arthritis. *Am J Pathol* **160:** 123–130

Resistance to endoplasmic reticulum stress is an acquired cellular characteristic of rheumatoid synovial cells

SATOSHI YAMASAKI[1], NAOKO YAGISHITA[1], KANEYUKI TSUCHIMOCHI[1,4], YUKIHIRO KATO[1], TAKESHI SASAKI[1], TETSUYA AMANO[1], MOROE BEPPU[3], HARUHITO AOKI[3], HIROSHI NAKAMURA[2], KUSUKI NISHIOKA[2] and TOSHIHIRO NAKAJIMA[1]

Departments of [1]Genome Science, and [2]Rheumatology, Immunology and Genetics Program, Institute of Medical Science, [3]Department of Orthopaedic Surgery, St. Marianna University School of Medicine, 2-16-1 Sugao, Miyamae-ku, Kawasaki, Kanagawa 216-8512; [4]Department of Orthopaedic Surgery, Kagoshima Graduate School of Medical and Dental Sciences, Kagoshima 890-8520, Japan

Received January 10, 2006; Accepted February 24, 2006

Abstract. Synoviolin is an endoplasmic reticulum (ER)-resident E3 ubiquitin ligase which plays a critical role in ER-associated degradation (ERAD). We found that Synoviolin is a novel causative factor for rheumatoid arthritis (RA), which is especially up-regulated in proliferating synovial cells in the disease. We attempted to examine the role of Synoviolin in ER stress-induced apoptosis and proliferation of synovial cells. RA synovial cells (RSCs) were refractory to ER stress-induced apoptosis compared with HEK293 or HeLa cells. RSCs were also more resistant to the apoptosis than synovial cells from osteoarthritis patients, significantly. Down-regulation of Synoviolin by siRNA increased the susceptibility to ER stress-induced apoptosis in RSCs. Knock-down of Synoviolin by siRNA did not only induce apoptosis of RSCs but also inhibited their proliferation *in vitro*. These data suggest that RSCs are extraordinarily refractory to ER stress-induced apoptosis, and we termed this special property 'hyper-ERAD'. Since Synoviolin is overexpressed in RSCs, and is known to play a critical role in the ERAD system as E3 ubiquitin ligase, hyper-ERAD is likely to present in these cells. Subsequently, the hyper-ERAD may cause synovial hyperplasia through its anti-apoptotic effect in RA. Further analyses are necessary to address this point, however, resistance to ER stress-induced apoptosis, or hyper-ERAD is a noteworthy new cellular characteristic of RSCs.

Correspondence to: Dr Toshihiro Nakajima, Department of Genome Science, Institute of Medical Science, St. Marianna University School of Medicine, 2-16-1 Sugao, Miyamae-ku, Kawasaki, Kanagawa 216-8512, Japan
E-mail: nakashit@marianna-u.ac.jp

Key words: Synoviolin, Hrd1, endoplasmic reticulum-associated degradation, apoptosis, proliferation

Introduction

Rheumatoid arthritis (RA) is characterized by abnormal immunity and synovial fibroblasts overgrowth followed by bone and cartilage destruction. While the immunological aspects of RA are well understood, the molecular basis for promoting overgrowth of rheumatoid synovial cells (RSCs) remains elusive (1,2). We recently succeeded in identifying Synoviolin as a possible pathogenic factor for RA (3). Synoviolin is an endoplasmic reticulum (ER)-resident ubiquitin ligase with N-terminal six transmembrane domains and RING finger motif (4,5). Synoviolin is involved in ER-associated degradation (ERAD), which is essential for maintenance of ER function, and activation of ERAD is important to eliminate proteins with an incorrect three-dimensional structure (unfolded protein) through the ubiquitin and proteasome system (3-6). The importance of Synoviolin in the ERAD system is clearly confirmed by this gene being embryonically lethal in the phenotypes of homozygous knock-out mice (3,7).

Both 'loss of function' and 'gain of function' using transgenic technology, Synoviolin is proved to be a pathogenic factor for arthropathy at least in mice (3). Detailed examination of synovial tissue from *synoviolin* heterozygous knock-out mice (*syno*$^{+/-}$) with collagen-induced arthritis (CIA) revealed that there is an aberrantly increased apoptosis of synovial cells, which inhibited the progression of synovial hyperplasia in the mice, in spite of comparable productions of anti-type II collagen antibodies, tumor necrosis factor α (TNFα), and interleukin 1 (IL-1) to those of wild-type mice. Conversely, there was remarkable synovial cell overgrowth in Synoviolin overexpressing mice. These results indicate that Synoviolin accelerates synovial cell overgrowth, and consequently leads to arthropathy in mice. Synoviolin overexpressing mice can be regarded as a novel RA model that firstly demonstrates the possible importance of hyperactivation of the ERAD system (hyper-ERAD) in overgrowth of RSCs, because RSCs express high levels of Synoviolin protein (3). To address this hypothesis, we examined whether RSCs are equipped with the hyper-ERAD system by Synoviolin, and

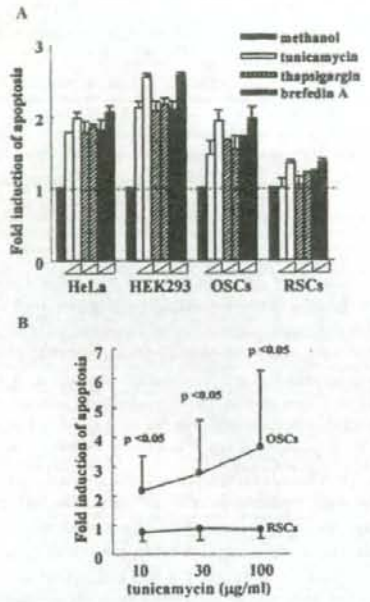

Figure 1. Rheumatoid synovial cells are refractory to ER stress-induced apoptosis. (A) HeLa, HEK293, and RSCs or OA synovial cells (OSCs) were treated with tunicamycin (10 or 100 μg/ml), thapsigargin (1 or 10 μM), breferdin A (10 or 100 μg/ml) or methanol (negative control) for 48 h. Apoptosis was evaluated using an ssDNA apoptosis ELISA kit. (B) RSCs (n=5) and OSCs (n=5) were treated with tunicamycin for 48 h. Apoptosis was evaluated by ssDNA Apoptosis ELISA kit.

how hyper-ERAD affects the proliferation and apoptosis of RSCs in this study.

Materials and methods

Reagents. ER stress inducers, including tunicamycin, thapsigargin and breferdin A, were obtained from Sigma (St. Louis, MO) to induce ER stress in various cells (8).

Synovial cell isolation and culture. Synovial cells were isolated from synovial tissue obtained from 10 patients with rheumatoid arthritis (RA) who met the American College of Rheumatology criteria for RA at the time of orthopedic surgery (9). In some experiments, synovial cells isolated from patients with osteoarthritis (OA) were also used. These cells were cultured in DMEM containing 1% penicillin, 1% streptomycin and 10% fetal bovine serum. The adherent synovial cells used in this study at third to fifth passages were <1% reactive with monoclonal antibodies, including CD3, CD68, CD20, and von Willebrand factor.

RNA interference assay. Small interfering RNA (siRNA) with 21 nucleotides was chemically synthesized (Hokkaido System Science Co., Japan). The siRNA for synoviolin was created by annealing 5'-CGU UCC UGG UAC GCC GUC ATT-3' (sense sequence) and 5'-UGA CGG CGU ACC AGG AAC GTT-3' (anti-sense). The sense sequence corresponds to the sequence of synoviolin cDNA (238-256), and the TT of 3' end is overhanging nucleotides. Transfection was carried out by using Oligofectamine (Invitrogen, CA) at the concentration of 20 nM annealed RNA duplex, according to the instructions provided by the supplier. The siRNA for green fluorescent protein (GFP) was used as negative control.

Western blot analysis. Cell cultures were harvested and lysed in buffer containing 25 mM Tris-HCl (pH 6.8), 50 mM NaCl, 1% NP-40, 0.25% SDS and protease inhibitors, and aliquots of clear cell lysates were separated on SDS-polyacrylamide gels, transferred onto nitrocellulose membrane, and immunoblotted with anti-Synoviolin monoclonal antibodies (Abs) (3). Bound antibodies were detected by peroxidase-conjugated goat anti-mouse Abs and ECL detection system (Amersham Pharmacia Biotech).

Apoptosis assay. Apoptosis of RSCs was determined using an ssDNA apoptosis ELISA kit (Chemicon International, Inc., CA). ELISA was carried out according to the manufacturer's protocol. The extent of apoptosis was evaluated as a fold induction compared with control cells. In some experiments, apoptosis was detected by staining cells with propidium iodide and analyzing them for DNA content on a FACScan to detect hypodiploid DNA.

Proliferation assay. The proliferation of RSCs was evaluated using Cell Counting Kit-8 (Dojindo, Kumamoto, Japan) according to the instructions provided by the manufacturer.

Statistical analysis. Data are expressed as mean ± SD. Differences between control and treated cells were examined for statistical significance using the Student's t-test. A P-value <0.05 denoted the presence of a statistically significant difference.

Ethical considerations. All human experimental protocols described in this study were approved by the Ethics Review Committees of St. Marianna University School of Medicine. Before obtaining human tissue, a signed consent form was obtained from each subject participating in the study.

Results

RSCs are refractory to ER stress-induced apoptosis. First, we simply questioned whether RSCs are refractory to apoptosis induced by excess accumulation of unfolded proteins in ER. RSCs are expected to have high ability to eliminate these unfolded proteins from ER through the 'hyper-ERAD' system by their high expression levels of Synoviolin. To address this issue, pharmacological analysis was performed by using ER stress inducers to evaluate the ERAD function of RSCs. We compared the sensitivities of RSCs to ER stress inducers with that of OA synovial cells (OSCs), human embryonic kidney (HEK293) cell, or HeLa cells, which are known to express a lower amount of Synoviolin (3; data not shown). These cells were treated with ER stress-inducing reagents (tunicamycin, thapsigargin and breferdin A) to load unfolded proteins in ER, and the susceptibility of these cells to ER stress-induced apoptosis was determined by ELISA. As expected, RSCs

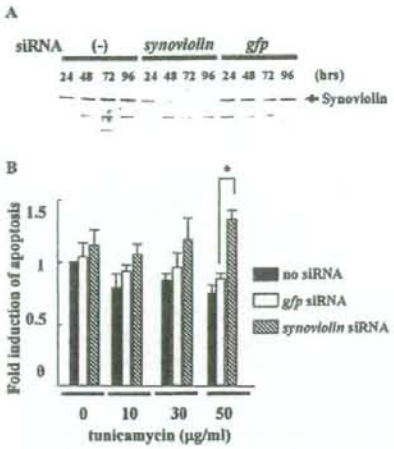

Figure 2. Synoviolin siRNA increase the sensitivity to ER stress-induced apoptosis. (A) Down-regulation of Synoviolin in RSCs by siRNA. (B) RSCs were treated with siRNA for 72 h, and the cells were further treated with an indicated dose of tunicamycin for 48 h. Apoptosis was evaluated by using ELISA. *P<0.05.

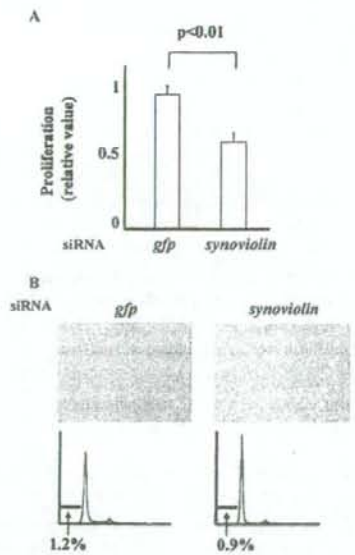

Figure 3. Down-regulation of Synoviolin inhibits RSC proliferation. (A) RSCs were treated with siRNA for 96 h, and the proliferation of the cells was evaluated using Cell Counting kit-8. (B) Morphological change (upper) and apoptosis assay (lower) of RSCs treated with siRNA for Synoviolin for 96 h. RSCs were treated with siRNA for 96 h, and the apoptosis of the cells was detected by FACScan after propidium iodide staining.

were found to be remarkably refractory to ER stress-induced apoptosis compared with OSCs, HEK293 cells or HeLa cells (Fig. 1A). Since RSCs were apparently more resistant to ER stress-induced apoptosis than OSCs, we further evaluated whether RSCs are more resistant to ER stress, and found that RSCs were more refractory to ER stress-induced apoptosis than OSCs, significantly (Fig. 1B; 10 μg/ml: RSCs 0.73±0.30, OSCs 2.18±1.19; 30 μg/ml: RSCs 0.84±0.35, OSCs 2.76±1.84; 100 μg/ml: RSCs 0.81±0.28, OSCs 3.65±2.53). It should be noted that apoptosis of RSCs was not induced at a considerably high concentration of tunicamycin (8). These data clearly indicate that RSCs are distinctly equipped with a high ability to deal with a large amount of unfolded proteins in ER.

Down-regulation of Synoviolin promotes ER stress-induced apoptosis of RSCs. Next, we addressed whether 'hyper-ERAD' is achieved by high expression of Synoviolin in RSCs. We administered an indicated dose of tunicamycin to RSCs after the down-regulation of Synoviolin expression by 72-h treatment with siRNA for Synoviolin. Treatment of RSCs with siRNA for Synoviolin efficiently suppressed the protein expression of Synoviolin (Fig. 2A). The siRNA for Synoviolin alone did not enhance the apoptosis of RSCs (Fig. 2B). Treatment with tunicamycin did not induce significant apoptosis again in RSCs treated with control siRNA. However, *synoviolin* knock-down significantly enhanced the apoptosis of RSCs induced by tunicamycin at a concentration of 50 μg/ml compared with those treated with control siRNA, even though the sensitivity of these cells to apoptosis is still very low compared with that of other cells (Fig. 2B). This data indicated that RSCs restored the sensitivity to ER stress-induced apoptosis by Synoviolin knock-down. Thus, it can be said that Synoviolin is important, at least in part, for the hyper-ERAD of RSCs, and for RSC survival in ER stress milieu.

Down-regulation of Synoviolin inhibits proliferation of RSCs. One of the most striking data of our previous report about Synoviolin is that Synovioin overexpressing mice develop arthropathy with synovial cell overgrowth. These results strongly suggest that Synoviolin is also required for synovial cell overgrowth. To verify the importance of Synoviolin in RSC proliferation, we carried out more detailed examinations of the proliferation of Synoviolin down-regulated RSCs. As we expected, the proliferation of RSCs was significantly inhibited by 96 h after treatment with siRNA for Synoviolin compared with RSCs treated with siRNA for GFP (Fig. 3A). Since the appearance of RSCs treated with siRNA for Synoviolin by phase contrast microscopic examination shows morphological change (Fig. 3B), we examined whether there are apoptotic cells in them by flow cytometry. There was no increment of hypodiproid DNA in Synoviolin down-regulated RSCs by 96-h treatment with siRNA for Synoviolin (Fig. 3B). These results are consistant with the data shown in Fig. 2B, and indicate that down-regulation of Synoviolin inhibits the proliferation of RSCs without inducing apoptosis of them.

Discussion

Based on our serial experiments, we propose 'hyper-ERAD' as a novel pathogenic mechanism that promotes RSC survival and proliferation, and that this machinery can be mediated by up-regulation of Synoviolin in RA. RSCs, equipped with

'hyper-ERAD', are proved to be a unique cell with high ability to accommodate severe ER stress (Fig. 1). Down-regulation of Synoviolin resulted in aberrant apoptosis of synovial cells in CIA-induced *syno*$^{+/-}$ mice (3). Likewise, down-regulation of the gene in RSCs resulted in increased apoptosis induced by ER stress inducers (Fig. 2). These accumulating data strongly support our novel disease concept that synovial cell overgrowth is triggered, at least in part, by hyper-ERAD, which consequently leads to synovial hyperplasia in RA. The importance of Synoviolin in 'hyper-ERAD' is also confirmed in this study.

Another remarkable aspect of Synoviolin is its ability to regulate the proliferation of synovial cells both *in vivo* and *in vitro*. Synoviolin overexpressing mice show spontaneous overgrowth of synovial cells (3), and siRNA for Synoviolin abrogates the proliferation of RSCs *in vitro* (Fig. 3). In addition, our recent analyses of the *synoviolin* promoter also demonstrated that transcriptional regulation of the gene is critical for cell growth and apoptosis *in vitro* (10), which strongly suggests that the amount of Synoviolin is critical to the regulation of synovial cell overgrowth.

Further examination is required to understand how Synoviolin regulates the proliferation of RSCs on a molecular basis. First, it is necessary to determine the alternation of unfolded protein response (UPR) by Synoviolin. It is believed that dual response UPR and the ERAD are triggered by the ER dysfunction or so-called 'ER stress', and both responses cooperate to maintain ER homeostasis (6,11). The ER-resident kinase, PKR-like ER kinase (PERK), is known to be activated as one UPR response. PERK phosphorylates the eukaryotic initiation factor (eIF2α) that attenuates global translation to block the influx of newly synthesized proteins into ER (12). Therefore, protein synthesis for cell proliferation becomes insufficient if the ERAD system does not work sufficiently enough to avoid ER stress and eventually triggers UPR. GADD153 is another candidate molecule that explains the importance of Synoviolin in RSC proliferation because it is thought to be activated in cells with ER stress, and causes cell cycle arrest (13). Actually, cell cycle study by staining cells with propidium iodide demonstrates that the cell treated with siRNA for Synoviolin seems to be arrested at G1 or G0 phase (Fig. 3B). Further detailed studies are necessary to clarify the whole mechanism of UPR activation in RSCs with Synoviolin down-regulation.

Is 'hyper-ERAD' really necessary for overgrowth of RSCs? It is easy to assume that 'hyper-ERAD' is a very favourable function for RSCs because the articular milieu in inflamed joints of RA is extremely hostile to ER. It is not difficult to find the cause of ER stress in inflamed joints of RA. For example, hypoxia frequently occurs in inflamed joints of RA, which is known to inhibit ER function (12). In addition, pro-inflammatory cytokines promote the synthesis of various proteins, including hyaluronate, cytokines and proteases in RSCs, which inevitably accelerates the accumulation of unfolded protein in ER. Indeed, nuclear translocation of ATF6, an ER-resident transcriptional factor that translocates to the nucleus under ER stress conditions (14), was certainly confirmed in RA synovia (data not shown). A report from another laboratory also implicates the existence of ER stress by demonstrating the high expression of BiP, a well-known transcriptional target for ATF6 (15). Thus, it is rational that 'hyper-ERAD' evoked by Synoviolin overexpression in RSCs helps RSCs to prevent these extra- and/or intra-cellular environmental stresses and subsequent apoptosis.

Here, we propose a concept that hyper-ERAD is a novel pathogenic factor for RA, which is especially important in RSC overgrowth. Historically, the autonomous proliferation of RSCs is thought to be due to high expression of proto-oncogenes, such as *c-myc*, *fos*, *ras*, or virus transforming gene *tax* or activation of specific transcriptional factors, such as NF-κB (16,17). Synoviolin is also a member of the genes responsible for synovial cell overgrowth. Moreover, Synoviolin is one of the most convincing molecules for the RA therapy targeting RSCs because it is an enzyme and enzymes are regarded as the most appropriate target for drug development. The detailed molecular mechanisms are still unclear and various approaches are required to prove our hypothesis; however, it should be noted that resistance to ER stress-induced apoptosis is a novel cellular characteristic of RSCs.

Acknowledgements

We thank Drs T. Ohta and K. Tanaka for the critical comments. We are grateful to S. Toriyama, N. Furuya, H. Takahashi, N. Takagi, M. Hinata, S. Shinkawa, A. Sugamiya, and Y. Nakagawa for the excellent technical assistance. This study was supported by LocomoGene Inc. and grants from Ministry of Education, Culture, Sports, Science and Technology, Japan Society for the Promotion of Science, Regional Science Promotion Program in Kanagawa, The Kanagawa High-Technology Foundation, Kanagawa Academy of Science and Technology Research Grants, Mochida Pharmaceutical Co., Ltd., Pharmaceuticals and Medical Devices Agency, and New Energy and Industrial Technology development organization.

References

1. Pap T, Muller-Ladner U, Gay RE and Gay S: Fibroblast biology. Role of synovial fibroblasts in the pathogenesis of rheumatoid arthritis. Arthritis Res 2: 361-367, 2000.
2. Szekanecz Z and Koch AE: Update on synovitis. Curr Rheumatol Rep 3: 53-63, 2001.
3. Amano T, Yamasaki S, Yagishita N, *et al*: Synoviolin/Hrd1, an E3 ubiquitin ligase, as a novel pathogenic factor for arthropathy. Genes Dev 17: 2436-2449, 2003.
4. Kaneko M, Ishiguro M, Niinuma Y, Uesugi M and Nomura Y: Human HRD1 protects against ER stress-induced apoptosis through ER-associated degradation. FEBS Lett 532: 147-152, 2002.
5. Bays NW, Gardner RG, Seelig LP, Joazeiro CA and Hampton RY: Hrd1p/Der3p is a membrane-anchored ubiquitin ligase required for ER-associated degradation. Nat Cell Biol 3: 24-29, 2001.
6. Kaufman RJ: Orchestrating the unfolded protein response in health and disease. J Clin Invest 110: 1389-1398, 2002.
7. Yagishita N, Ohneda K, Amano T, *et al*: Essential role of synoviolin in embryogenesis. J Biol Chem 280: 7909-7916, 2005.
8. Chae HJ, Kim HR, Xu C, *et al*: BI-1 regulates an apoptosis pathway linked to endoplasmic reticulum stress. Mol Cell 15: 355-366, 2004.
9. Arnett FC, Edworthy SM, Bloch DA, *et al*: The American Rheumatism Association 1987 revised criteria for the classification of rheumatoid arthritis. Arthritis Rheum 31: 315-324, 1988.
10. Tsuchimochi K, Yagishita N, Yamasaki S, *et al*: Identification of a crucial site for synoviolin expression. Mol Cell Biol 16: 7344-7356, 2005.
11. Friedlander R, Jarosch E, Urban J, Volkwein C and Sommer T: A regulatory link between ER-associated protein degradation and the unfolded-protein response. Nat Cell Biol 2: 379-384, 2000.

12. Koumenis C, Naczki C, Koritzinsky M, *et al*: Regulation of protein synthesis by hypoxia via activation of the endoplasmic reticulum kinase PERK and phosphorylation of the translation initiation factor eIF2alpha. Mol Cell Biol 22: 7405-7416, 2002.
13. Barone MV, Crozat A, Tabaee A, Philipson L and Ron D: CHOP (GADD153) and its oncogenic variant, TLS-CHOP, have opposing effects on the induction of G1/S arrest. Genes Dev 8: 453-464, 1994.
14. Shuda M, Kondoh N, Imazeki N, *et al*: Activation of the ATF6, XBP1 and grp78 genes in human hepatocellular carcinoma: a possible involvement of the ER stress pathway in hepatocarcinogenesis. J Hepatol 38: 605-614, 2003.
15. Blass S, Union A, Raymackers J, *et al*: The stress protein BiP is overexpressed and is a major B and T cell target in rheumatoid arthritis. Arthritis Rheum 44: 761-771, 2001.
16. Qu Z, Garcia CH, O'Rourke LM, Planck SR, Kohli M and Rosenbaum JT: Local proliferation of fibroblast-like synoviocytes contributes to synovial hyperplasia. Results of proliferating cell nuclear antigen/cyclin, c-myc, and nucleolar organizer region staining. Arthritis Rheum 37: 212-220, 1994.
17. Nakajima T, Aono H, Hasunuma T, *et al*: Overgrowth of human synovial cells driven by the human T cell leukemia virus type I tax gene. J Clin Invest 92: 186-193, 1993.

ARTHRITIS & RHEUMATISM
Vol. 54, No. 3, March 2006, pp 808–817
DOI 10.1002/art.21638

Comparative Analysis of Gene Expression Profiles in Intact and Damaged Regions of Human Osteoarthritic Cartilage

Tomoo Sato,[1] Koji Konomi,[2] Satoshi Yamasaki,[1] Satoko Aratani,[1] Kaneyuki Tsuchimochi,[3] Masahiro Yokouchi,[4] Kayo Masuko-Hongo,[1] Naoko Yagishita,[1] Hiroshi Nakamura,[1] Setsuro Komiya,[4] Moroe Beppu,[1] Haruhito Aoki,[1] Kusuki Nishioka,[1] and Toshihiro Nakajima[1]

Objective. **To analyze the differences in gene expression profiles of chondrocytes in intact and damaged regions of cartilage from the same knee joint of patients with osteoarthritis (OA) of the knee.**

Methods. **We compared messenger RNA expression profiles in regions of intact and damaged cartilage (classified according to the Mankin scale) obtained from patients with knee OA. Five pairs of intact and damaged regions of OA cartilage were evaluated by oligonucleotide array analysis using a double in vitro transcription amplification technique. The microarray data were confirmed by real-time quantitative polymerase chain reaction (PCR) amplification and were compared with previously published data.**

Results. **About 1,500 transcripts, which corresponded to 8% of the expressed transcripts, showed ≥2-fold differences in expression between the cartilage tissue pairs. Approximately 10% of these transcripts (n = 151) were commonly expressed in the 5 patient samples. Accordingly, 114 genes (35 genes expressed in intact > damaged; 79 genes expressed in intact < damaged) were selected. The expression of some genes related to the wound-healing process, including cell proliferation and interstitial collagen synthesis, was higher in damaged regions than in intact regions, similar to the findings for genes that inhibit matrix degradation. Comparisons of the real-time quantitative PCR data with the previously reported data support the validity of our microarray data.**

Conclusion. **Differences between intact and damaged regions of OA cartilage exhibited a similar pattern among the 5 patients examined, indicating the presence of common mechanisms that contribute to cartilage destruction. Elucidation of this mechanism is important for the development of effective treatments for OA.**

Osteoarthritis (OA) is the most prevalent form of arthritis in the elderly and is characterized primarily by the degeneration and loss of articular cartilage. OA is considered a heterogeneous group of disorders with a variety of pathogenic factors, all of which result in similar patterns of cartilage degeneration (1). In OA of the knee, the medial compartment of the articular cartilage is the most susceptible to degeneration, whereas the lateral compartment remains relatively unaffected (2). This phenomenon appears in a single joint despite the same OA susceptibility of the cartilage matrix and the same genetic background.

There is now abundant evidence that chondrocytes play a critical role in cartilage degeneration. For example, OA chondrocytes secrete a variety of matrix breakdown products and cytokines, and cleavage of type II collagen is observed primarily around chondrocytes (3). Therefore, changes in the gene expression patterns of chondrocytes in response to various exogenous stimuli could affect the integrity of articular cartilage. Based on

Supported in part by Santen Pharmaceutical Company Ltd., the Japanese Ministry of Education, Science, Culture, and Sports, the Japanese Ministry of Health and Welfare, the Japan Science and Technology Corporation, the Kanagawa Academy of Science and Technology, and the Japan College of Rheumatology.

[1]Tomoo Sato, MD, PhD, Satoshi Yamasaki, MD, PhD, Satoko Aratani, PhD, Kayo Masuko-Hongo, MD, PhD, Naoko Yagishita, MS, Hiroshi Nakamura, MD, PhD, Moroe Beppu, MD, PhD, Haruhito Aoki, MD, PhD, Kusuki Nishioka, MD, PhD, Toshihiro Nakajima, MD, PhD: St. Marianna University School of Medicine, Kawasaki, Japan; [2]Koji Konomi, PhD: Santen Pharmaceutical Company Ltd., Osaka, Japan, and St. Marianna University School of Medicine, Kawasaki, Japan; [3]Kaneyuki Tsuchimochi, MD, PhD: Kagoshima University, Kagoshima, Japan, and St. Marianna University School of Medicine, Kawasaki, Japan; [4]Masahiro Yokouchi, MD, PhD, Setsuro Komiya, MD, PhD: Kagoshima University, Kagoshima, Japan.

Address correspondence and reprint requests to Toshihiro Nakajima, MD, PhD, Institute of Medical Science, St. Marianna University School of Medicine, 2-16-1 Sugao Miyamae-ku, Kawasaki 216-8512, Japan. E-mail: nakashit@marianna-u.ac.jp.

Submitted for publication January 5, 2005; accepted in revised form November 10, 2005.

this concept, many groups of investigators have reported that gene expression in certain molecules differ from region to region within a single OA joint (4–7).

Because comprehensive gene expression profiles in intact and damaged regions of human OA cartilage have never been compared, the following questions remain unresolved. What percentage of the expressed transcripts shows obvious differences in expression levels in intact and damaged regions? What percentage of the differentially expressed transcripts shows the same expression pattern in different patient samples? What are the molecular functions involved in such groups of genes?

To provide answers to these questions, we used Affymetrix high-density oligonucleotide array analysis to compare the gene expression profile of chondrocytes in intact regions of joint cartilage with the profile of chondrocytes in damaged regions of joint cartilage from the same knee. We also evaluated the validity of our oligonucleotide array data according to the results of real-time quantitative polymerase chain reaction (PCR) amplification as well as gene expression data reported by other groups of investigators (4–7).

MATERIALS AND METHODS

Cartilage samples. Specimens of human articular cartilage were obtained from a total of 15 OA patients; 5 of the initial 9 patients' samples were used for microarray analysis, based on the results of the histologic assessment, and 4 of the 6 patients' samples used to confirm the microarray results were used for real-time PCR analysis after histologic assessment. Patients were undergoing total knee replacement surgery at St. Marianna University Hospital. OA was diagnosed according to the findings of the clinical history and physical examination, as well as radiographic findings. Within 4 hours after surgery, 8 pieces of cartilage tissue (4 apparently intact cartilage pieces and 4 damaged cartilage pieces) were dissected from each specimen. Each piece of cartilage was further divided into 2 fragments. One of the fragments was rapidly frozen in liquid nitrogen and stored at –80°C until RNA isolation was performed. The other fragment was frozen in TissueTek OCT compound (Sakura, Tokyo, Japan) and was used for histologic examination.

This study was performed after obtaining approval from the Ethics Committee for Human Studies, St. Marianna University Hospital. All patients provided informed consent.

Histopathologic assessment. Cartilage sections were stained with Safranin O–fast green. Sections were then evaluated histopathologically and scored according to the Mankin scale (8), which assesses the following 4 features: cartilage structure (0–6 scale, where 0 = normal, 1 = surface irregularity, 2 = pannus and surface irregularity, 3 = clefts to transitional zone, 4 = clefts to radial zone, 5 = clefts to calcified zone, and 6 = complete disorganization), cellularity (0–3 scale, where 0 = normal, 1 = hypercellularity, 2 = cloning, and 3 = hypocellularity), Safranin O staining (0–4 scale, where 0 = normal, 1 = slight reduction, 2 = modest reduction, 3 = severe reduction, and 4 = no dye noted), and tidemark integrity (0–1 scale, where 0 = intact and 1 = blood vessels cross the tidemark). Cartilage sections in the present study were scored for the first 3 features (structure, cellularity, and Safranin O staining). Analysis of tidemark integrity was not evaluated because of the absence of a calcified zone in the cartilage samples we examined.

Based on the Mankin scores, we defined intact and damaged regions of the OA cartilage samples for comparative analysis. Intact cartilage regions were defined as follows: normal cartilage structure (score of 0), no cell clusters (score of 0 or 1), and a total score <4. Damaged cartilage regions were defined as follows: clefts within the cartilage structure (score of 3 or 4), presence of several cell clusters (score of 2), and a total score >6. Of the 9 pairs of cartilage samples obtained, 5 met these definitions. These paired samples were obtained from 5 OA patients (4 women and 1 man; age range 64–81 years). For real-time quantitative PCR, 4 of 6 additional pairs of cartilage samples met the above definitions. These additional samples were obtained from another group of 4 OA patients (4 women; age range 64–74 years).

RNA extraction. Frozen cartilage tissue (~50 mg) was rapidly minced with ophthalmic scissors in 1 ml of Isogen (Nippon Gene, Tokyo, Japan) and then immediately homogenized using a Polytron homogenizer (Hitachi Koki, Tokyo, Japan). Total RNA was isolated from the homogenized solution according to the manufacturer's instructions, except that the aqueous phase after initial separation was mixed with 0.25 ml of isopropanol, 0.25 ml of a high-salt precipitation solution (1.2*M* NaCl and 0.8*M* sodium citrate), and 3 μl of Ethachinmate (Nippon Gene) instead of with 0.5 ml of isopropanol. This extraction process was performed once again before RNA cleanup and DNase digestion using the RNeasy Mini kit (Qiagen, Crawley, UK).

Normalization of the amount of RNA. Because the amount of total RNA obtained from the piece of cartilage tissue was too small to measure accurately using a spectrophotometer, a Human β-Actin Competitive PCR Set (Takara Bio, Kyoto, Japan) was used according to the manufacturer's instructions to normalize the RNA amount that would be available for microarray analysis. Total RNA isolated from cultured chondrocytes was used as a control. To confirm the integrity of the total RNA, 60 ng (normalized value) of denatured total RNA was loaded in each lane of a 1% nondenaturing (formaldehyde-free) agarose gel, subjected to electrophoresis, and stained with ethidium bromide (data not shown). Smaller amounts of total RNA can be detected in nondenaturing agarose gels than in formaldehyde-denaturing agarose gels.

High-density oligonucleotide array analysis. Because the amount of RNA was too small to be applied to the standard protocol of the GeneChip system (Affymetrix, Santa Clara, CA), we used a double in vitro transcription technique, which can amplify the signals considerably. Biotin-labeled complementary RNA (cRNA) fragments were prepared as the target hybridized to the oligonucleotide array according to the Affymetrix protocol (GeneChip Eukaryotic Small Sample Target Labeling Technical Note). Briefly, double-stranded complementary DNA (cDNA) was synthesized from 50 ng (nor-

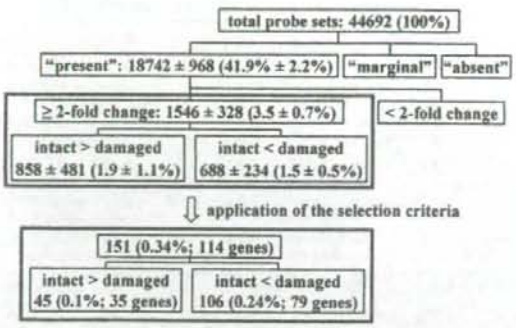

Figure 1. Flow chart showing the procedure for identifying genes with different expression levels in intact and damaged regions of human osteoarthritic cartilage. The terms "present," "marginal," and "absent" represent expression levels of the transcripts described in Materials and Methods. Values are the mean ± SD number and percentage of transcripts. See Materials and Methods for details of the selection criteria.

malized value) of total RNA as the starting material. The cDNA was amplified by initial in vitro transcription, resulting in unlabeled cRNA. Double-stranded cDNA was also synthesized from the amplified cRNA. A second in vitro transcription was performed to produce biotin-labeled cRNA from the double-stranded cDNA. The biotin-labeled cRNA was fragmented before hybridization. Finally, 15 μg of the fragmented cRNA was hybridized to human U133A and U133B arrays, stained with streptavidin–phycoerythrin, and scanned with a GeneArray scanner.

Analysis of the data. We normalized all intensity data by scaling the average signal intensity of 100 maintenance genes on each array to a value of 2,000 and then determined whether the transcript was detected ("present"), undetected ("absent"), or at the limit of detection ("marginal") using Microarray Suite 5.0 software (Affymetrix). Comparison analysis was performed using Data Mining Tool 3.0 software (Affymetrix).

To identify the genes that showed the same expression pattern in different samples, the selection criteria (Figure 1) were defined as follows. First, selected transcripts had to show a ≥2-fold difference in the level of expression among all 5 samples or a ≥3-fold difference among 4 of the 5 samples. Second, selected transcripts had to be detected ("present") and have normalized signal intensities >100 in either the intact or the damaged region. The "fold change" value represents the ratio of the average signal intensity in intact regions to the average signal intensity in damaged regions of all 5 samples. The standard error of the mean was calculated from the standard deviation of the fold change value and was determined by applying to the following formula each mean and SD of the signal intensities in the intact and damaged regions of all 5 samples:

$$CV = \sqrt{CV1^2 + CV2^2}$$

where CV represents the coefficient of variation (the SD divided by the mean), CV1 represents the CV of the signal intensities in intact regions, and CV2 represents the CV of the signal intensities in damaged regions.

The significance of the difference in levels of expression between the intact and damaged groups of cartilage was determined by paired *t*-test. Hierarchical clustering analysis was performed using the Cluster and TreeView software from Stanford University (available at http://rana.lbl.gov/EisenSoftware.htm).

Real-time quantitative PCR. Total RNA was prepared in the same way as for the oligonucleotide array analysis. These RNA samples were converted into cDNA using Superscript II reverse transcriptase (Invitrogen, Carlsbad, CA) and random primer. Quantitative PCR reactions were performed using the ABI 7500 Real-Time PCR system (Applied Biosystems, Foster City, CA) according to the manufacturer's instructions. Primer and probe sets were purchased as TaqMan Gene Expression Assays for the set of genes to be studied: Hs00248808 (*CHRDL2*), Hs00234422 (*MMP2*), Hs00155794 (*APOD*), Hs00182807 (*FGF13*), Hs00243202 (*S100A4*), Hs00932737 (*TGFBI*), Hs00610420 (*PTGES*), and Hs00200180 (*TNFAIP6*). The quantities of target genes were calculated using the standard curve method and were normalized with 18S RNA (ABI item no. 4319413E) as an internal control. The fold change and SEM values were calculated as described above.

RESULTS

Findings of the histopathologic assessment of cartilage samples. First, we evaluated histopathologically the dissected cartilage fragments and scored them using the Mankin scale. We then determined whether each cartilage fragment satisfied the criteria for intact or damaged tissue as defined in Materials and Methods. Briefly, cartilage samples with a smooth surface and hyaline cartilage architecture and without fibrocartilage were defined as an intact region of OA cartilage. Cartilage samples with fibrillation, clefts, and several cell clusters were defined as a damaged region of OA cartilage. The histologic score for the damaged region (mean ± SD 7.8 ± 0.8) was significantly higher than that for the intact region (2.6 ± 0.5).

Findings of the genome-wide screening. We used the Affymetrix GeneChip system to compare gene expression profiles in intact and damaged regions of the same OA knee joint. There are 44,692 probe sets on the Affymetrix human U133 chip set, covering >39,000 transcript variants that represent 33,000 human genes. The expression analysis detected ~40% (mean ± SD 18,742 ± 968) of all probe sets corresponding to the transcripts in each cartilage sample (Figure 1), but little difference was noted between the percentage of transcripts expressed in intact and damaged regions of cartilage (intact 42.1 ± 2.5% [18,813 ± 1,106] versus damaged 41.8 ± 2.1% [18,671 ± 933]). About 3.5% (1,546 ± 328) of all probe sets indicated a ≥2-fold difference in expression per sample (intact > damaged

Table 1. Representative genes with higher expression in intact regions than in damaged regions of human osteoarthritic cartilage*

Category, gene name	Gene symbol	Public ID	Fold change	SEM	P†
Transcription factors					
v-*ets* erythroblastosis virus E26 oncogene homolog 1	*ETS1*	NM_005238	3.64	1.35	0.007
Signal transduction					
Guanylate cyclase 1, soluble, α3 subunit	*GUCY1A3*	NM_000856	8.17	2.60	0.028
Membrane proteins/receptors					
Glypican 5	*GPC5*	NM_004466	4.82	1.46	0.010
Transporters/carrier proteins					
Apolipoprotein D	*APOD*	NM_001647	6.24	1.15	0.004
Cytokines/growth factors					
Fibroblast growth factor 13	*FGF13*	NM_004114	4.47	0.73	0.001
Proteases					
Matrix metalloproteinase 2	*MMP2*	NM_004530	7.30	2.90	0.017
Secreted inhibitors/antagonists					
Chordin-like 2	*CHRDL2*	NM_015424	8.95	5.35	0.060
Immunity/defense					
Complement component 4 binding protein α subunit	*C4BPA*	NM_000715	6.44	3.53	0.121
Extracellular matrix proteins					
Vitrin	*VIT*	NM_053276	9.34	3.09	0.031
Miscellaneous					
Expressed sequence tag	*EST*	BF002625	14.01	6.14	0.056

* See Materials and Methods for the definition of "fold change" and for the method of calculating the SEM. Complete data for all of the selected genes are available upon request from the corresponding author. Public ID = accession number in public databases (RefSeq or GenBank).
† All *P* values were significant (<0.05), as determined by paired *t*-test, except for the *P* values for genes *CHRDL2, C4BPA,* and *EST*.

Table 2. Representative genes with higher expression in damaged regions than in intact regions of human osteoarthritic cartilage*

Category, gene name	Gene symbol	Public ID	Fold change	SEM	P†
Transcription factor					
Sex determining region Y–type high mobility group box 11	*SOX11*	NM_003108	30.19	7.66	0.009
Cell cycle					
Cyclin D1	*CCND1*	NM_053056	6.96	2.25	0.006
Metabolism					
Phosphoserine aminotransferase 1	*PSAT1*	NM_058179	9.82	4.77	0.009
Collagen synthesis					
Prolyl 4-hydroxylase α polypeptide III	*P4HA3*	NM_182904	9.66	3.44	0.021
Transporters/carrier proteins					
Uncoupling protein 2	*UCP2*	NM_003355	10.56	5.88	0.017
Glycosylation					
UDP-*N*-acetyl-α-D-galactosamine:polypeptide *N*-acetylgalactosaminyltransferase–like 1	*GALNTL1*	XM_031104	12.16	2.97	0.010
Cell motility/invasion					
S100 calcium binding protein A4	*S100A4*	NM_002961	5.33	1.73	0.007
Signal transduction					
Down syndrome critical region gene 1	*DSCR1*	NM_004414	4.69	0.82	0.008
Membrane proteins/receptors					
Triggering receptor expressed on myeloid cells 1	*TREM1*	NM_018643	15.38	4.43	0.020
Secreted inhibitors/antagonists					
Tumor necrosis factor α–induced protein 6	*TNFAIP6*	NM_007115	25.34	5.78	0.001
Growth factors/cytokines					
Cytokine receptor–like factor 1	*CRLF1*	NM_004750	22.90	7.98	0.031
Immunity/defense					
Prostaglandin E synthase	*PTGES*	NM_004878	12.44	3.08	0.013
Proteases					
A disintegrin and metalloproteinase domain 12	*ADAM12*	NM_003474	4.43	1.59	0.024
Structural proteins					
Erythrocyte membrane protein band 4.1–like 3	*EPB41L3*	NM_012307	5.36	2.88	0.070
Adhesion proteins					
Transforming growth factor β–induced 68 kd	*TGFBI*	NM_000358	12.05	3.74	0.001
Extracellular matrix proteins					
C-type lectin domain family 3, member B	*CLEC3B*	NM_003278	11.16	5.45	0.030
Miscellaneous					
Hypothetical protein FLJ37034	*FLJ37034*	H16258	7.65	2.46	0.019

* See Materials and Methods for the definition of "fold change" and for the method of calculating the SEM. Complete data for all of the selected genes are available upon request from the corresponding author. Public ID = accession number in public databases (RefSeq or GenBank).
† All *P* values were significant (<0.05), as determined by paired *t*-test, except for the *P* value for gene *EPB41L3*.

1.9 ± 1.1% [858 ± 481]; intact < damaged 1.5 ± 0.5% [688 ± 234]). This corresponds to ~8% of the expressed transcripts (1,546/18,742 = 0.082). Furthermore, ~10% of differentially expressed transcripts were commonly detected in all 5 OA samples (151/1,546 = 0.098).

Thus, we identified 114 genes, which consisted of 35 genes expressed in intact > damaged cartilage and 79 genes expressed in intact < damaged cartilage. These genes were then subdivided into functional categories: the 35 genes with higher expression in intact regions than in damaged regions were subdivided into 10 categories, and the 79 genes with higher expression in damaged regions than in intact regions were subdivided into 17 categories. Since ~18% of all selected genes (21 of 114) have unknown function, these were assigned to the miscellaneous group, representing the largest category in the list. (Complete data for all of the selected genes are available upon request from the corresponding author.)

Differentially expressed genes in intact versus damaged regions. Tables 1 and 2 show a representative gene from each functional subcategory: 10 genes that were highly expressed in intact regions and 17 genes that were highly expressed in damaged regions, respectively.

The following genes were highly expressed in the intact region of OA cartilage (Table 1). The v-Ets-1 erythroblastosis virus E26 oncogene homolog (*ETS1*; 3.64-fold) is a member of the Ets transcription factor family and can activate the expression of many matrix metalloproteinases (MMPs) (9,10). Soluble guanylate cyclase 1α3 subunit (*GUCY1A3*; 8.17-fold) functions as the main receptor for nitric oxide. Glypican 5 (*GPC5*; 4.82-fold) is a glycosyl phosphatidylinositol (GPI)–anchored heparan sulfate proteoglycan and functions as a "coreceptor" for several "heparin-binding" growth factors (11). Apolipoprotein D (*APOD*; 6.24-fold) is a member of the lipocalin superfamily of transporter proteins that bind progesterone and arachidonic acid (12). Fibroblast growth factor 13 (*FGF13*; 4.47-fold), which is also called fibroblast growth factor homologous factor 2, is an intracellular protein that unlike other FGFs, cannot activate any FGF receptors (13). MMP-2 (*MMP2*; 7.3-fold) is an enzyme known to degrade denatured collagen. Chordin-like 2 (*CHRDL2*; 8.95-fold) is a novel chordin-like bone morphogenetic protein inhibitor expressed preferentially in chondrocytes of developing cartilage and OA cartilage (14). C4 binding protein α subunit (*C4BPA*; 6.44-fold) is a regulatory protein of the classical pathway of complement. Vitrin (*VIT*; 9.34-fold) is a member of the von Willebrand factor A superfamily, and it might serve as a bridge between collagen fibrils and the hyaluronan network (15). The function of gene BF002625 (14.01-fold) remains unknown. Hierarchical clustering of this group of miscellaneous genes did not show characteristic changes (Figure 2A).

The following genes were highly expressed in the damaged region of OA cartilage (Table 2). Sex determining region Y–type high mobility group box 11 (*SOX11*; 30.19-fold) plays an important role in tissue remodeling, including craniofacial and skeletal tissue remodeling (16). Cyclin D1 (*CCND1*; 6.96-fold) is an essential component of chondrocyte proliferation in the growth plate (17). Phosphoserine aminotransferase 1 (*PSAT*; 9.82-fold) is an enzyme involved in the biosynthesis of L-serine, and the messenger RNA (mRNA) level for *PSAT* appears to be up-regulated to support cell proliferation (18). Prolyl 4-hydroxylase α polypeptide III (*P4HA3*; 9.66-fold) is a component of prolyl 4-hydroxylase, a key enzyme in collagen synthesis (19). Uncoupling protein 2 (*UCP2*; 10.56-fold) is a mitochondrial anion carrier protein that also protects against oxidative stress–induced cell death (20). Polypeptide *N*-acetylgalactosaminyltransferase–like 1 (*GALNTL1*; 12.16-fold) is an enzyme that catalyzes the initial reaction in the biosynthesis of *O*-linked oligosaccharide. S100 calcium binding protein A4 (*S100A4*; 5.33-fold) is involved in cell proliferation and tumor metastasis (21). Down syndrome critical region gene 1 (*DSCR1*; 4.69-fold) acts as a negative regulator of calcineurin signaling, which is known to induce chondrogenesis (22,23). Triggering receptor expressed on myeloid cells 1 (*TREM1*; 15.38-fold) plays a role in acute inflammation. Tumor necrosis factor α–induced protein 6 (*TNFAIP6*; 25.34-fold) forms complexes with inter-α-inhibitor (a serine protease inhibitor) and inhibits MMP activation via antiplasmin activity (24,25). Cytokine receptor–like factor 1 (*CRLF1*; 22.9-fold) is expressed in chondrocytes and osteoblasts and plays a role in cartilage and bone formation (26). Prostaglandin E (PGE) synthase (*PTGES*; 12.44-fold), which is also called microsomal PGE synthase 1 (27), is responsible for the production of PGE_2, which has a wide variety of biologic activities. A disintegrin and metalloproteinase domain 12 (*ADAM12*; 4.43-fold) is one of the candidate genes in OA susceptibility and progression (28). Erythrocyte membrane protein band 4.1–like 3 (*EPB41L3*; 5.36-fold) is a structural protein that links transmembrane proteins to the actin cytoskeleton. Transforming growth factor β–induced 68 kd (*TGFBI*; 12.05-fold) may play an important role in cell–collagen interactions in cartilage (29). C-type lectin domain family 3, member B (*COLEC3B*; 11.16-fold) is a plasminogen-binding protein that plays a role in tissue

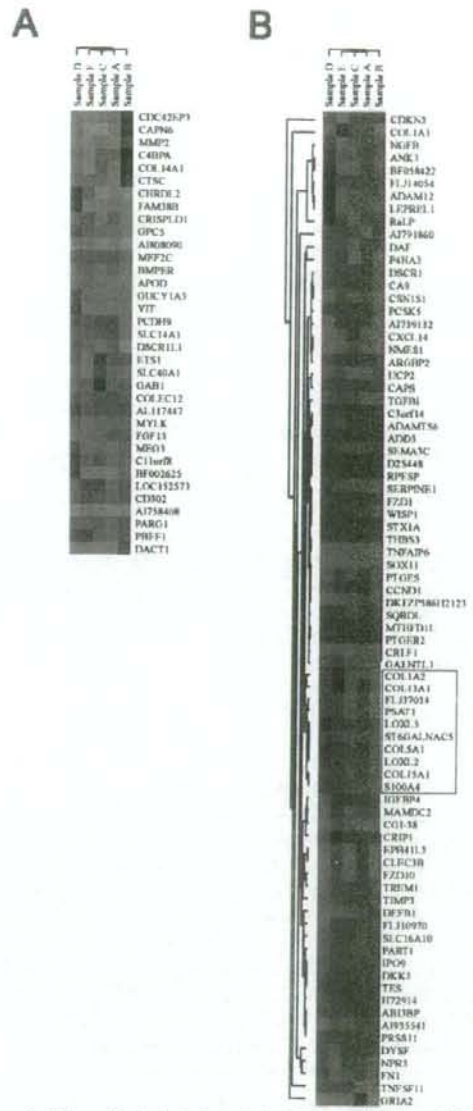

Figure 2. Hierarchical clustering of **A**, 35 genes that were highly expressed in intact regions of human osteoarthritic (OA) cartilage (green) and **B**, 79 genes that were highly expressed in damaged regions of human OA cartilage (red). Black areas indicate no difference in the level of expression between intact and damaged regions of human OA cartilage.

growth and remodeling (30). The function of gene FLJ37034 (7.65-fold) remains unknown.

There is a characteristic change in the group of genes with higher expression in damaged cartilage. Three interstitial collagen genes (collagen, type I, α1 [*COL1A1*]; collagen, type I, α2 [*COL1A2*]; and collagen, type V, α1 [*COL5A1*]) together with 4 collagen biosynthetic enzymes (*P4HA3* [19]; lysyl oxidase–like 2 [*LOXL2*] [31]; leprecan-like 1 [*LEPREL1*] [32], and *LOXL3* [33]) were expressed at significantly higher levels in chondrocytes from the damaged region of OA cartilage than those from the intact region (Complete data for all of the selected genes are available upon request from the corresponding author.) Furthermore, hierarchical clustering analysis indicated that *COL1A2*, *COL5A1*, *LOXL2*, and *LOXL3* as well as other minor collagen genes belonged to the same cluster in the tree diagram (Figure 2B). This cluster also contained 2 proliferation-associated genes (*S100A4* and *PSAT1*).

Results of real-time quantitative PCR of selected 8 genes. To validate the oligonucleotide array data, real-time quantitative PCR was performed on 8 selected genes using additional 4 pairs of cartilage samples (Figure 3). For these 8 genes, the region of high expression as determined by real-time quantitative PCR was consistent with the region of high expression as determined by oligonucleotide array analysis. We found that the levels of expression of mRNA for *FGF13*, *TGFBI*, *PTGES*, and *TNFAIP6* genes in intact and damaged regions of OA cartilage were significantly different as determined by both methods. In the present study, however, the fold change in gene expression estimated using real-time quantitative PCR tended to

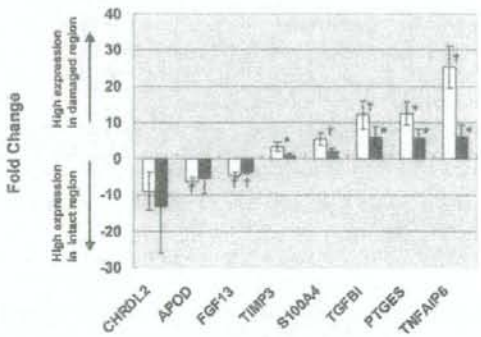

Figure 3. Histogram showing levels of expression of 8 selected genes, as measured by oligonucleotide array (open bars; n = 5) and real-time quantitative polymerase chain reaction (solid bars; n = 4). Values are the mean ± SEM (see Materials and Methods for further details). * = $P < 0.05$; † = $P < 0.01$ for intact region versus damaged region, by paired *t*-test.